FABRICATION AND STUDY OF THE ELECTRICAL PROPERTIES OF Cu – Cu_2O PHOTOELECTROCHEMICAL SOLAR CELL WITH VARYING ELECTROLYTES;

BY

MUHAMMAD ABDULRAHMAN
(SPS/13/MPY/00022)
(BSc. Physics)

A DISSERTATION SUBMITTED TO THE DEPARTMENT OF PHYSICS, BAYERO UNIVERSITY, KANO, IN PARTIAL FULFILMENT OF THE REQUIREMENTS FOR THE AWARD OF THE DEGREE MASTER OF SCIENCE (M.Sc.) IN PHYSICS.

OCTOBER, 2016.

DECLARATION

I hereby declare that this work is the product of my research efforts undertaken under the supervision of Prof A.O Musa and has not been presented anywhere for the award of a degree or certificate. All the sources have been duly acknowledged.

MUHAMMAD ABDULRAHMAN

(SPS/13/MPY/00022)

CERTIFICATION

This is to certify the research work for this dissertation and the subsequent write-up by Muhammad Abdulrahman (SPS/13/MPY/00022) were carried out under my supervision.

Prof. A.O Musa

(Supervisor)

Dr. T.H. Darma

(Head of Department)

APPROVAL PAGE

This has been examined and approved for the award of masters of Science degree in Physics.

_____

Prof. Nasiru Rabiu

(External Examiner)

_____

Dr. Abdu Yunusa

(Internal Examiner)

_____

Prof A.O Musa

(Supervisor)

_____

Dr. T.H. Darma

(Head of Department)

_____

Dr. B. I. Tijjani

(PG Coordinator)

ACKNOWLEDGMENT

I start by giving thanks to Almighty ALLAH for keeping me alive and giving me opportunity to complete this programme successfully.

I will like to express my gratitude to Prof. A.O. Musa for his invaluable advice, inspiration and support throughout my study. Without his enlightenment and his guidance this work will not have been completed and what he has taught me is greatly helpful not only in my carrier but for my whole life.

I am very grateful to my internal examiner Dr. Abdu Yunusa for his encouragement and support. I also appreciate the support of my colleague Ibrahim Garba Shitu for his assistance and sacrifices in times of difficulties.

My special thanks go to my mother Dr. Fatima Salman Koki, Khadija Musa Shanono and Malam Aminu Maitama for helping me to fulfill my dreams. This acknowledgement is incomplete without mentioning my uncles Alhaji Muhammad Rabi'u, Alhaji Liman, Alhaji Ahmad Garba (Tomy).

I give thanks and appreciation to my uncle Chief Imam of Hadejia Malam Yusuf Abdulrahman and Engr. Rabi'u Garba for their kindness, prayer, love and moral support during my study period.

DEDICATION

This project work is dedicated to my late father Alhaji Kawu Abubakar Barde, my lovely mom Hajiya Fatima Abdulrahman and my wife to be Fatima Abdullahi.

TABLE OF CONTENTS

Declaration i

Certification ii

Approval page iii

Acknowledgment iv

Dedication v

Table of contents vi

List of figures ix

List of Tables xi

Abstract xiii

CHAPTER ONE

1.0 Introduction 1

1.1 History of photovoltaic cells 4

1.2 Photovoltaic system 7

1.3 Aims and objectives 8

1.4 Scope of the research 9

CHAPTER TWO

2.0 Introduction 10

2.1 Theoretical consideration 12

2.2 Solar cells 15

2.2.1 Types of Solar cells 15

2.2.2 Principle operation of solar cell 16

2.2.3 Current voltage (I-V) characteristic 17

2.3 solar cell parameter 18

2.3.1 The light generating current density, J_l 18

2.3.2 The short circuit current density, J_{sc} 19

2.3.3 The open-circuit voltage, V_{oc} 20

2.3.4 Non-ideality factor, A 20

2.3.5 The dark saturated current density, j_o 20

2.3.6 Power conversion efficiency 21

2.4 Theoretical determination of solar cell electrical parameters 21

2.5 Defects in Cu_2O 21

2.6 Method of production of Cu_2O 22

2.6.1 Thermal oxidation 22

2.6.2 Electro-deposition 23

2.6.3 Sputtering 23

2.6.4 Chemical bath deposition 24

2.7 Fabrication of heterojunction solar cells 25

2.8 Fabrication of homojunction solar cells 26

2.9 Performance of cu_2o solar cells 27

CHAPTER THREE

3.0 Introduction 31

3.1 Cutting and cleaning the sample 31

3.2 Oxidation 31

3.3 Chemical etching 32

3.4 Cell fabrication 33

3.5 Measurement of open circuit voltage and short circuit current 34

CHAPTER FOUR

4.1 Results 35

4.2 Discussions 47

CHAPTER FIVE

5.0 Summary 51

5.1 Conclusion 52

References 52

Appendix 56

LIST OF FIGURES

Figure 2.1: A p-n junction in thermal equilibrium with zero bias voltage applied.

Figure 2.2: Photo electrochemical reactions at the semiconductor/electrolyte interface for (a) n-type semiconductor, and (b) p-type semiconductor

Figure2.3: Current/voltage characteristic of a solar cell (a) in the dark, and (b) under illumination

Figure 2.4: Equivalent circuit of an ideal solar cell

Figure 3.1: Block diagram of the etching process

Figure 3.2: Illustration of the fabricated Cu – Cu_2O Photoelectrochemical solar cell.

Figure 3.3: Circuit diagram of I-V Characteristic Measurement

Figure 4.1: The I – V characteristic of the PEC device under illumination using $FeCl_3$ electrolyte

Figure 4.2: The I – V characteristic of the PEC device under illumination using NaCl electrolyte

Figure 4.3: The I – V characteristic of the PEC device under illumination using $BaCl_2$ electrolyte

Figure 4.4: The I – V characteristic of the PEC device under illumination using $MgCl_2$ electrolyte

Figure 4.5: The I – V characteristic of the PEC device under illumination using$MgSO_4$ electrolyte

Figure 4.6: The I – V characteristic of the PEC device under illumination using KI electrolyte

Figure 4.7: The I – V characteristic of the PEC device under illumination using $FeSO_4$ electrolyte

Figure 4.8: The I – V characteristic of the PEC device under illumination using $CaSO_4$ electrolyte

Figure 4.9:The I – V characteristic of the PEC device under illumination using $ZnSO_4$ electrolyte

Figure 4.10: The I – V characteristic of the PEC device under illumination using $NiSO_4$ electrolyte

Figure 4.11: The I – V characteristic of the PEC device under illumination using $CuSO_4$ electrolyte

Figure 4.12: The I – V characteristic of the PEC device under illumination using $CoCl_2$ electrolyte

Figure 4.13:The I – V characteristic of the PEC device under illumination using NaCl and $MgCl_2$ electrolyte

Figure 4.14: The I – V characteristic of the PEC device under illumination using $FeCl_3$ and $NiSO_4$ electrolyte

Figure 4.15: The I – V characteristic of the PEC device under illumination using $NiSO_4$ and $BaCl_2$ electrolyte

Figure 4.16: The I – V characteristic of the PEC device under illumination using $FeCl_3$ and $BaCl_2$ electrolyte

Figure 4.17: The I – V characteristic of the PEC device under illumination using $CoCl_2$ and KI electrolyte

Figure 4.18: The I – V characteristic of the PEC device under illumination using NaCl, $MgCl_2$ and $ZnSO_4$ electrolyte

Figure 4.19: The I – V characteristic of the PEC device under illumination using $FeSO_4$, $NiSO_4$ and $BaCl_2$ electrolyte

Figure 4.20: The I – V characteristic of the PEC device under illumination using NaCl, MgCl2, ZnSO4 and $CaSO_4$ electrolyte

Figure 4.21:The I – V characteristic of the PEC device under illumination using $FeSO_4$, $NiSO_4$, $BaCl_2$ and NaCl electrolyte

Figure 4.22: The I – V characteristic of the PEC device under illumination using $FeSO_4$, $NiSO_4$, $BaCl_2$, NaCl and $MgSO_4$ electrolyte

LIST OF TABLES

Table 1 for $FeCl_3$ electrolyte

Table 2 for $CuSO_4$ electrolyte

Table 3 for $CoCl_2$ and KI electrolyte

Table 4 for NaCl, $MgCl_2$, $ZnSO_4$ and $CaSO_4$ electrolyte

Table 5 for NaCl, $MgCl_2$ and $ZnSO_4$ electrolyte

Table 6 for NaCl electrolyte

Table 7 for KI electrolyte

Table 8 for $FeSO_4$ electrolyte

Table 9 for BaCl electrolyte

Table 10 for $CaSO_4$ electrolyte

Table 11 for $MgSO_4$ electrolyte

Table 12 for $MgCl_2$ electrolyte

Table 13 for CoCl electrolyte

Table 14 for $NiSO_4$ electrolyte

Table 15 for $ZnSO_4$ electrolyte

Table 16 for NaCl and MgCL electrolyte

Table 17 for NaCl,$MgCl_2$ and $ZnSO_4$ electrolyte

Table 18 for NaCl,$MgCl_2$,$ZnSO_4$ and $CaSO_4$ electrolyte

Table 19 for $NiSO_4$ and $Bacl_2$ electrolyte

Table 20 for $FeSO_4$,$NiSO_4$ and $BaCl_2$ electrolyte

Table 21 for $FeSO_4$, $NiSO_4$,$BaCl_2$ and NaCl electrolyte

Table 22 for $FeSO_4$,$NiSO_4$,$BaCl_2$, NaCl and $MgSO_4$ electrolyte

Table 23 for $FeCl_3$ and $BaCl_2$ electrolyte

Table 24 for $NiSO_4$ electrolyte

ABSTRACT

Copper (I) oxide is prepared by partial thermal oxidation of copper foils at 950°C and used it as one of the electrode while pure copper foil is used as the second electrode (counter electrode). The PEC device is contained in a transparent cylindrical plastic container using some selected electrolytes (NaCl, $FeCl_3$, $NiSO_4$, $BaCl_3$, KI,. etc). The I – V characteristic curves were plotted for the various PEC and the maximum power points P_{max} were recorded. The highest values were obtained for the PEC device containing $FeCl_3$ electrolyte, an open circuit voltage V_{oc}, of 119.1mV, a short circuit current I_{sc}, of 1080.4μA, a fill-factor, FF, of 0.82 and a maximum power point P_{max}, of 1.06×10^{-4} W were obtained for $FeCl_3$ electrolyte respectively.

CHAPTER ONE

INTRODUCTION

1.0 INTRODUCTION

It is expected that the global energy demand will be doubled within the next 60 years. Fossil fuels, however, are running out and are held responsible for the increased concentration of carbon dioxide in the earth's atmosphere. Hence, developing environmentally friendly renewable energy is one of the challenges to society in the 21st century. Ever-increasing world energy demand, depleting non-renewable energy resources and disruptive climate change due to greenhouse gases has aroused much interest in alternative renewable energy sources. Solar energy is one of the best available alternatives, for it is both abundant and clean. All wind, fossil fuel, hydro and biomass energy have their origins in sunlight. Solar energy falls on the surface of the earth at a rate of 120 petawatts, (1 petawatt = 1015 watt). This means all the solar energy received from the sun in one days can satisfied the whole world's demand for more than 20 years. A solar cell is an electrical device that converts the energy of light (solar energy) directly into electricity by the photovoltaic effect (Miyake, *et al*., 2010). The photovoltaic effect was discovered by Becquerel in 1839, but it was until the 1950s that a semiconductor device for converting sunlight energy into electrical energy was developed. Since then, such devices have evolved, and nowadays solar cells are made of different materials and structures. Although most of the semiconductor materials exhibit the photovoltaic effect, they should have a bandgap greater than 1.0 eV to be suitable for practical solar cells.

Discovery of photovoltaic effect in silicon (Si) diode in 1954 dawned the era of modern solid state photovoltaic (PV) technology. Since then Si solar cells have evolved as the most mature photovoltaic technology and represent over 90% of the present day photovoltaic market worldwide. The PV market is mushrooming at a rate of 48% since 2002 and is the world's fastest growing energy technology. In spite of this tremendous growth in PV sector, energy from PV technology accounts for less than 0.1% of the world energy demand. The primary reason for this is high module and installation costs of silicon photovoltaics. There is a strong need for the development of photovoltaic cells with low cost, high efficiency, and good stability. In the past decade a new class of photovoltaics based on organic materials has emerged and are a promising alternative to inorganic solar cells because of their low processing cost, ease of processibility, roll-to-roll processiblity for large area devices and mechanical flexibility (Miyake, *et al*., 2010)

Among the available alternative sources of energy, the sun appears more promising. The solar energy is emitted primarily as electromagnetic radiation in the ultraviolet to infrared and spectral regions (0.2-3μm). The sun is predicted to have a reasonable life-time, with a projected constant radiative energy output of over 10 billion (10^{10}) years (Sze, 1981).

This research focuses attention on direct conversion of solar energy to electricity, using photovoltaic (PV) cells. The direct conversion of solar energy to electricity is likely to be a good solution to the global energy problem; especially if practical

economic means of direct conversion can be developed. Africa having enjoyable high level of insolation most times of the year stands to benefit a lot from solar photovoltaic technology.

Photovoltaic systems have several advantages; they are cost effective alternative in areas where extending utility power line is very expensive; they have no moving parts and require little maintenance; and they produce electricity without polluting the environment.

There are presently few PV cells that are widely used in commercial quantities. These are silicon pn-junction solar cells, cadmium sulphide/copper sulphide (Cds/Cu_2S), gallium arsenide (GaAs) and amorphous silicon (a-Si) solar cells. But their future development is predictably going to be lowered by high cost of material and fabrication methods. For large scale power generation using these cells But their future development is predictably going to be lowered by high cost of material and fabrication methods. For large scale power generation using these cells, there should be a drastic reduction in the cost of the cells. Photoelectrochemical solar cells (PEC) of copper (I) oxide (Cu_2O) is studied in this work because of the low cost and non – toxic nature of the materials used. Copper (I) oxide is prepared by partial thermal oxidation of copper foils at 950°C and used as one electrode while pure copper foil is used as the counter electrode. The PEC device is contained in a transparent cylindrical plastic container using some selected electrolytes (NaCl, $FeCl_3$, $NiSO_4$, $BaCl_3$, KI…). The I – V characteristic curves were plotted for the various PEC and the maximum

power points P_{max} were recorded.

1.1 HISTORY OF PHOTOVOLTAIC CELLS

The term ‘photovoltaic’ emerge from the Greek: phos meaning ‘light’ and ‘voltaic’ cannoting electrical, from the name of the Italian physicist Volta, after whom the measurement unit volt is name.

The most significant usage solar power has found has been in electrical energy generation. The previous century has witnessed a plethora of advancements in the processes of using solar energy in the form of electrical energy. The discovery of the phenomenon known as the photovoltaic effect enabled this conversion of the two forms of energy. It was first recorded by Alexandre-Edmund Becquerel in 1839. He observed that the application of light on platinum electrode coated with silver in an electrolyte produced electric current. This marked the first time in history when electricity was produced by the effect of light. His apparatus consisted of two electrodes of the same metal such as platinum, gold or brass - metals are chemically inactive in electrolyte consisting of dissociative ions. The electrolytes used were dilute acids and ionic solutions. This simple setup, albeit similar to a chemical galvanic cell functioned in the exact option. Electric current was produced not by electrolysis, but by a combination of the photovoltaic effect and ionic conductivity in the electrolyte.

However, it was until 1883 that the first solar cell was built by Charles Fritts, who coated the semiconductor selenium with an extremely thin layer of gold to form the junctions (Mairaj, *et al.*, 2010).

The 20th century saw development of new ideas and more discoveries. The discovery of the photoelectric effect by Albert Einstein in 1905 explained the physics behind the photovoltaic effect. Towards the millennium mark, the world saw a great need for sources of renewable energy that do not contribute towards negative environmental impact and slow down the depletion of natural resources. Several key concepts that help explain the theory of the photovoltaic effect include the photoelectric effect and PN junction theory. A completely new area of study today focuses on solar power and photovoltaic (PV) technologies.

Similar effect for the case of selenium was observed in 1876, by Adams and Day (Green, 1982, Musa, 1995). However, not until 1883 that first solar cell was built by Charles Fritt, an American scientist who coated the semiconductor selenium with an extremely thin layer of gold to form a junction. Photosensitivity of a combination of copper-cuprous oxide structure was reported in 1904 by Hallwachs (Musa, 1995). The First silicon solar cell was made in 1941, by Russell Ohl (Musa, 1995).

In 1954 Chapin, Pearson and Fuller produced the first practical solar cells with a sunlight energy conversion efficiency of 6%, at Bell laboratory. Continuous improvement in the fabrication technology, more understanding of the theory of the device operation and improved design of the device resulted in gradually increasing efficiency which reached approximately 14% in terrestrial sunlight by Jenny et al 1958 (Musa 1995). Even though low efficiency GaAs solar cells was reported much earlier, Zhores Alferov and others in 1970 created the first highly effected GaAs

heterostructure solar cells in USSR. Production equipment was not developed until early 1980s, limiting the ability of companies to manufacture the GaAs solar cells (Musa, 1995).

Prior to 1950, photovoltaic devices were limited in use to highly specialized applications, such as light metering, where electrical current demand was minimal.

The advent of silicon junction technology in the 1950's permitted the development of high cost, high conversion efficiency silicon homojunction photovoltaic cells. The devices have been used with considerable success in the space program where cost is of little significance. However, the cost of such devices as energy generators is high for terrestrial applications wherein they must compete against conventional generators. Much of the cost is as a result of the high quality standards required for space craft components and also to the high cost of preparing silicon crystals of the required purity. The solar grade silicon (crystalline silicon) is often made using Czochralski process and this tends to be expensive (Musa, 1995).

However, photovoltaic systems are capable of transforming one kilowatt of solar energy falling on one square meter into about a hundred watts of electricity. One hundred watts can power most household appliances. Standard solar cells covering the sun-facing roof space of a typical home can provide about 8500-kilowatt-hour of electricity annually, which is about the average household's yearly electric consumption (Musa, 1995).

A comprehensive review of accomplishments and difficulties encountered by

researchers in the area of Cu_2O based solar cells is given in chapter 2.

1.2 PHOTOVOLTAIC SYSTEM

A photovoltaic system (PV system) is a system which uses one or more solar panels modules to convert sunlight into electricity. It consists of multiple components, including the photovoltaic modules, mechanical and electrical connections mountings and means of regulating or conditioning of the electrical output.

The photovoltaic effect whose acronym is PV can be defined as a process by which a voltage is produced at the junction of two different materials (e.g. a metal semi conductor contact or a p - n junction) through an incident proton e.m.f and the ability to deliver power to a load, the primary power coming from the sun. Energy conversion device, which are used to convert sunlight to electricity by the used of the photovoltaic effect, are called photovoltaic cells or solar cells.

The explanation for the photovoltaic effect lies on the ideas from quantum theory. Light is made up of packet of energy called photons, whose energy depends only upon the frequency or colour of the light. The energy of the visible photons is sufficient to excite electron bound into solids up to higher energy levels where the are freer to move. The science luminary in person of Einstein showed through his experiment in 1905 reason for blue or ultraviolet light to provide enough energy for electron for electron to escape completely from the surface of matter and the light is absorbed, photon rare given to excite electrons to higher energy state within the material, but the excited electrons quickly relax back to their ground state. The built-in asymmetry

pulls the excited electron away before they relax and feeds them to an external circuit in photovoltaic effect. The additional energy of the excited electron give rise to potential barrier of electromotive force (e.m.f.) and derives the electron through a load in the external circuit to perform electrical work (Musa, 2010). These studies justify the selection of an appropriate electrolyte for Photoelectrochemical solar cell work.

1.3 AIM AND OBJECTIVES

The aim of this research is to fabricate a Cu – Cu_2O Photoelectrochemical solar cell and to study the I–V characteristic curves with change in the electrolytes used.

The objectives of the study are:

(i) To use mixtures of these electrolytes in the cell.

(ii) To study the I–V characteristics of both the single electrolytes and the mixtures of these electrolytes used.

(iii) To extract the internal and the external parameters of the solar cells from these I–V characteristic curves.

(iv) To use the extracted parameters for the calculation of the electrical power conversion efficiencies of the PEC devices.

(v) To study the effect of the various electrolytes on the electrical power conversion efficiencies.

1.4 SCOPE OF THE RESEARCH

The work shall be limited to fabrication and studying the electrical properties of Cu – Cu_2O Photoelectrochemical solar cell with different electrolyte such as NaCl, $CuSO_4$, KI, $FeCl_3$, FeSO4, $BaCl_2$, $CaSO_4$, $MgSO_4$, $MgCl_2$, $CoCl_2$, $ZnSO_4$, etc.

CHAPETER TWO

LITERATURE REVIEW

2.0 INTRODUCTION

A solar cell is an electronic device which directly converts solar radiation energy into electricity in the process called photovoltaic effect. Light shining on the solar cell create an electrical current or voltage in material which generate electric power. Key factors of this process are the intensity of radiation, the spectral distribution of radiation, light absorption material and design of the external circuit. A variety of materials can potentially satisfy the requirements for photovoltaic energy conversion, however for efficient photovoltaic energy conversion, semiconductor materials in the form of a *p*-*n* junction are essential.

When light strikes material, the incident photons with an energy greater than that of the band gap will excite a negatively charged electron from low energy state (valence band) to a higher energy state (conduction band) leaving behind a passivity charged vacancy (a hole) therefore creating electron-hole pairs. However these generated electron-hole pairs will only exist, for a length of time equal to the minority carrier lifetime before they recombine. If the incident photons have energy lower than that of the band gap the electron energy state will not changed and will immediately relax down and recombine with the hole and the energy will be lost as heat and no current or power can be generated (Seyed, 2013).

The generated electron-hole pairs should be separated and collected before recombination by the action of the electric field. This electric field is created by joining *n*-type and *p*-type semiconductor materials and forming a *p*-*n* junction. A *p*–*n* junction is created by doping, or

growing a layer of crystal doped with one type of dopant on top of a layer of crystal doped with another type of dopant. Since the *n*-type region has a high electron concentration and the *p*-type a high hole concentration, after joining *p*-type and *n*-type semiconductors, electrons near the *p–n* interface tend to diffuse from the *n*-type side to the *p*-type side leaving leave holes, positively charged ions, in the *n* region. Similarly, holes flow by diffusion from the *p*-type side to the *n*-type side leaving electrons, negatively charged ions, in the *p* region. Therefore on the *n*-type side, positive ion cores are exposed and on the *p*-type side, negative ion cores are exposed. This will create charged regions and hence internal electrical field nearby the *p–n* interfaces. The electrical field will sweeps out the free carries (electrons and holes) and accelerates them in opposite directions causing the depletion of carries, hence, forming the depletion layer or space charge region (Fig. 2.1).

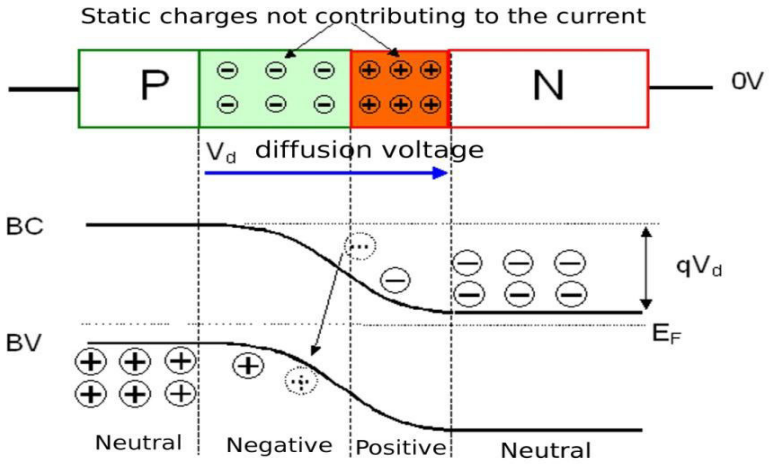

Figure 2.1 A p-n junction in thermal equilibrium with zero bias voltage applied.

If the light-generated minority carriers survive long enough to reaches the *p-n* junction, it is swept across the junction by the electric field at the junction, where it is now a majority carrier which is then carried towards the contacts terminals creating voltage difference on either side of

the photovoltaic cell. The magnitude of this voltage drop is called the open circuit voltage and scales with the intensity of light while remains constant with time for a given intensity. If the terminals of the solar cell are connected together, the light-generated carriers can flow through the external circuit. The higher the open circuit voltage is, the better is the quality of the photovoltaic cell, and hence the more efficient will be the solar cell in converting light into electrical energy (Seyed, 2013).

The ratio of the number of carriers collected by the solar cell to the number of photons of a given energy incident on the solar cell is called quantum efficiency and it can be expressed either as a function of wavelength or as energy. It is one at the particular wavelength if all photons of that wavelength are absorbed and the resulting minority carriers are collected and it is zero for photons with energy below the band gap. However, the quantum efficiency for most solar cells is reduced because of the effects of recombination, where charge carriers are not able to move into an external circuit. The impact of surface passivation and diffusion length on collection probability is important. It is more favorable to place *p*-*n* junction closer to surface rather than bulk, thus the separated carriers have a shorter distance to travel within the cell and as a result a lower chance of recombining.

2.1 THEORETICAL CONSIDERATION

The theory of solar cells explains the process by which light energy in photons is converted into electric current when the photons strike a suitable semiconductor device. The theoretical studies predict the fundamental limits of solar cell, and give guidance on the phenomena that contribute to losses and solar cell efficiency.

Solar photovoltaic energy conversion is used today for both space and terrestrial energy generation. The success of solar cells in space application is well known (e.g., communication satellites, manned and unmanned space exploration). On earth are water pumping, transport, telephone communication etc. (Musa, 2010).

However, the need for much more extensive use of solar cells in terrestrial applications is becoming clearer with growing understanding of the true cost of fossil fuels and with the widespread demand for renewable and environmentally acceptable terrestrial energy resources (Stephen, 2010).

This section explains the nature of the photovoltaic energy conversion principle involved in the Cu – Cu_2O photoelectrochemical solar cells. The relevant solar cell current-voltage equation and those used for the calculation of the fill-factor and the electrical power conversion efficiency of the fabricated solar cell are given.

In photoelectrochemical solar cells light is absorbed by a semiconductor immersed in an electrolyte solution. Charge separation takes place at the semiconductor electrolyte interface with the electron or hole stimulating an electron – transfer (redox) reaction at the surface. There are two fundamental types of photo-electrochemical cells; liquid – junction photovoltaic cells to convert light to electricity and photo electrolysis cells in which some of the light energy is used to drive a chemical reaction up hill in energy thus functioning as a type of solar battery.

The light sensitive electrode in the photoelectrochemical solar cell is conceptually equivalent to a schottky barrier solar cell such as the metal – insulator – semiconductor (MIS) solar cell, since the conduction and valence bands bends at the semiconductor – electrolyte interface (see figure 2.2). The barrier thus formed creates a space charge layer which separates the light generated

holes and electrons. If the semiconductor is n-type, the bands bend upwards at the surface (see figure 2.2a) and hence holes migrate to the surface on illumination. On the other hand, if the semiconductor is p-type, the bands bend downwards at the surface (figure2.2b). N-type semiconductors induce photo oxidation of suitable solutes in the electrolyte while p-type semiconductors induce photo reduction. As shown in figure 2.2, the electrochemical potential of the components in the electrolyte must be well matched to the semiconductor band edges.

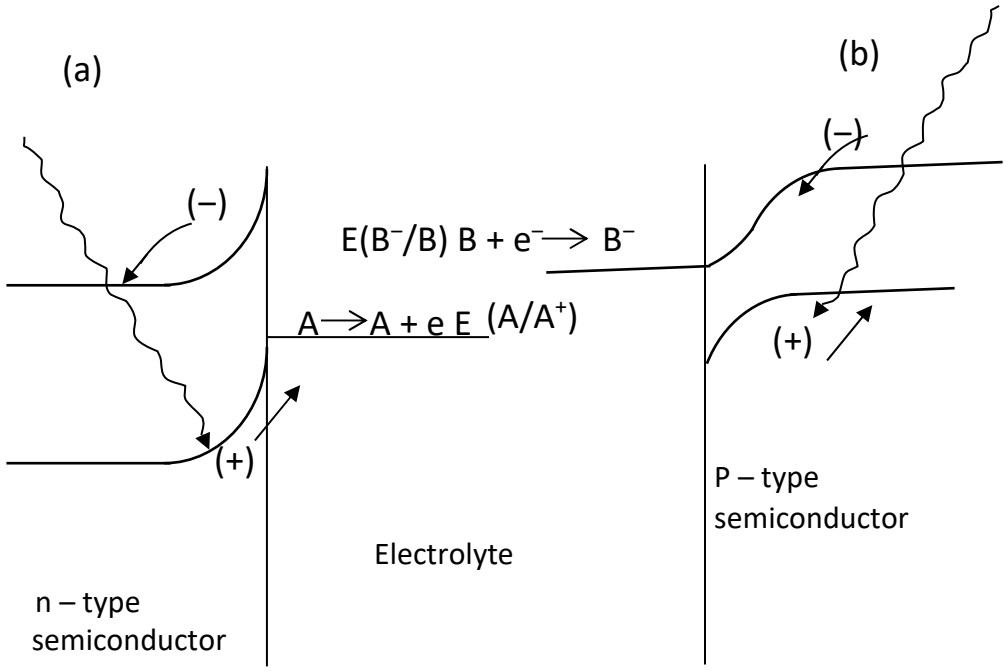

Figure 2.2: **Photo electrochemical reactions at the semiconductor/electrolyte interface for (a) n-type semiconductor, and (b) p-type semiconductor**

In liquid-junction photovoltaic solar cells the electron-transfer (redox) component generated in solution (A^+ in figure 2.2a or B^- in figure 2.2b) migrates to a counter electrode where it is converted back to A or B, respectively. Hence the electrolyte simply serves as a conductor to remove charge from the interface and to complete the electrical circuit (Musa and Yunusa, 2013).

The major electrical parameters of a solar cell can be analyzed by studying its current voltage characteristics under illumination and in the dark. These parameters provide the output performance of solar cells.

2.2 SOLAR CELLS

Solar cells are devices that can convert the energy of the sun directly into electricity and can provide nearly permanent power at low operating cost, and is virtually free of pollution.

Solar cells at present furnish the most important long duration power supply for satellite and space vehicles. Such cells have also been successfully employed in small-scale terrestrial applications. As the worldwide energy demand increases conventional energy resources such as burning coal and other fossil fuels, will be exhausted in the not – too distant future and they also produce carbon dioxide, the main gas responsible for global warming. Since sunlight is clean, abundant and effectively limitless, solar cells are a non - polluting and renewable alternative to more conventional energy sources. Moreover, since there are no moving parts solar cells continue to operate reliable for many years without maintenance.

2.2.1 Types of solar cells

There are three (3) types of solar cells (i) Homojunction (ii) Heterojunction (iii) Metal-Semiconductor

Homojunction: Is a semiconductor interface that occurs between layers of similar semiconductor material, these materials have equal band gaps but typically have different doping. In most practical cases a homojunction occurs at the interface between an n-type (donor doped) and p-type (acceptor doped) semiconductor such as silicon, this is called a p-n junction. Examples of homojunction solar cells are; Silicon (Si), GaAs, and CdTe (Musa, 2010).

Heterojunction: Is the interface that occurs between two layers or region of dissimilar crystalline semiconductors. These semiconducting materials have unequal band gaps as opposed to a homojunction. Examples of heterojunction solar cells are; ZnO/Cu_2O, Cu_2O/Cu_2S, CuO/Cu_2O (Musa, 2010).

Metal – semiconductor junction: (M-S) junction is a type of junction in which a metal comes in contact with a semiconductor device M-S junctions can either be rectifying or non-rectifying. The rectifying metal semiconductor junction forms a schottky barrier, making a device known as schottky diode, while the non-rectifying junction is called an ohmic contact. Examples of m-s semiconductor are; Cu/Cu_2O, Zn/Cu_2O (Musa, 2010)

There are a variety of types of solar cells under development. Despite the complicated fabrication process and high cost the majority of solar cells fabricated today are silicon-based solar cells. Silicon-based solar cells types are single crystalline, large-grained poly crystalline and amorphous forms and they dominated PV market by taking 85% of share (Avrutin*, et al.*, 2011).

These are some reviews of the actual work conducted by the researches on PEC solar cells in the field, the size of the sample is 1cm × 1cm, $I_{sc} = 280\mu A$, $V_{oc} = 60mV$, $\eta = 0.62 \times 10^{-2}$ %; $I_{sc} = 370\mu A$, $V_{oc} = 70.4mV$, $\eta = 1.07 \times 10^{-2}$%; $I_{sc} = 423\mu A$, $V_{oc} = 73.6mV$, $\eta = 1.31 \times 10^{-2}$% (Oamen, *et al.* 2013);the size of the sample is 3cm × 3cm $I_{sc} = 423\mu A$, $V_{oc} = 73.6mV$, $\eta = 1.31 \times 10^{-2}$% (Musa and Yunusa, 2013).

2.2.2 Principle of operation of a solar cell

A solar cell consists of a potential energy barrier within a semiconductor material that is capable of separating the electrons and holes that are generated by the absorption of light within the

semiconductor (Musa, 2010). A typical solar cell is a P-N junction. The junction is formed by bringing two semi-conducting material with different electrical properties into a close contact. Then a diffusion of electron occurs from the region of high electron concentration (the n-type side of the junction) into the region of low electron concentration (P-type side of the junction). When the electrons diffuse across the P-N junction, they recombine with holes on the P-type side. The diffusion of carries does not happen indefinitely however, because of an electric field which is created by the imbalance of charge immediately on either side of the junction which the diffusion creates. The electric field established across the P-n junction creates a diode that promotes current to the flow in only one direction across the junction.

2.2.3 Current voltage (I-V) characteristic

The main electric parameters of a solar cell can be analyzed by studying its current voltage characteristics under illumination and in the dark. These parameters are:

(a) The short circuit current (J_{sc})

(b) The open circuit voltage (V_{oc})

(c) The fill factor (FF)

(d) The dark saturation current density (J_o)

(e) The diode non ideality factor (A) and

(f) The power conversion efficiency (η)

There parameters provide the output performance of a solar cell. Figure 2.3 illustrates the J - V characteristic of a solar cell showing some of the parameters listed above.

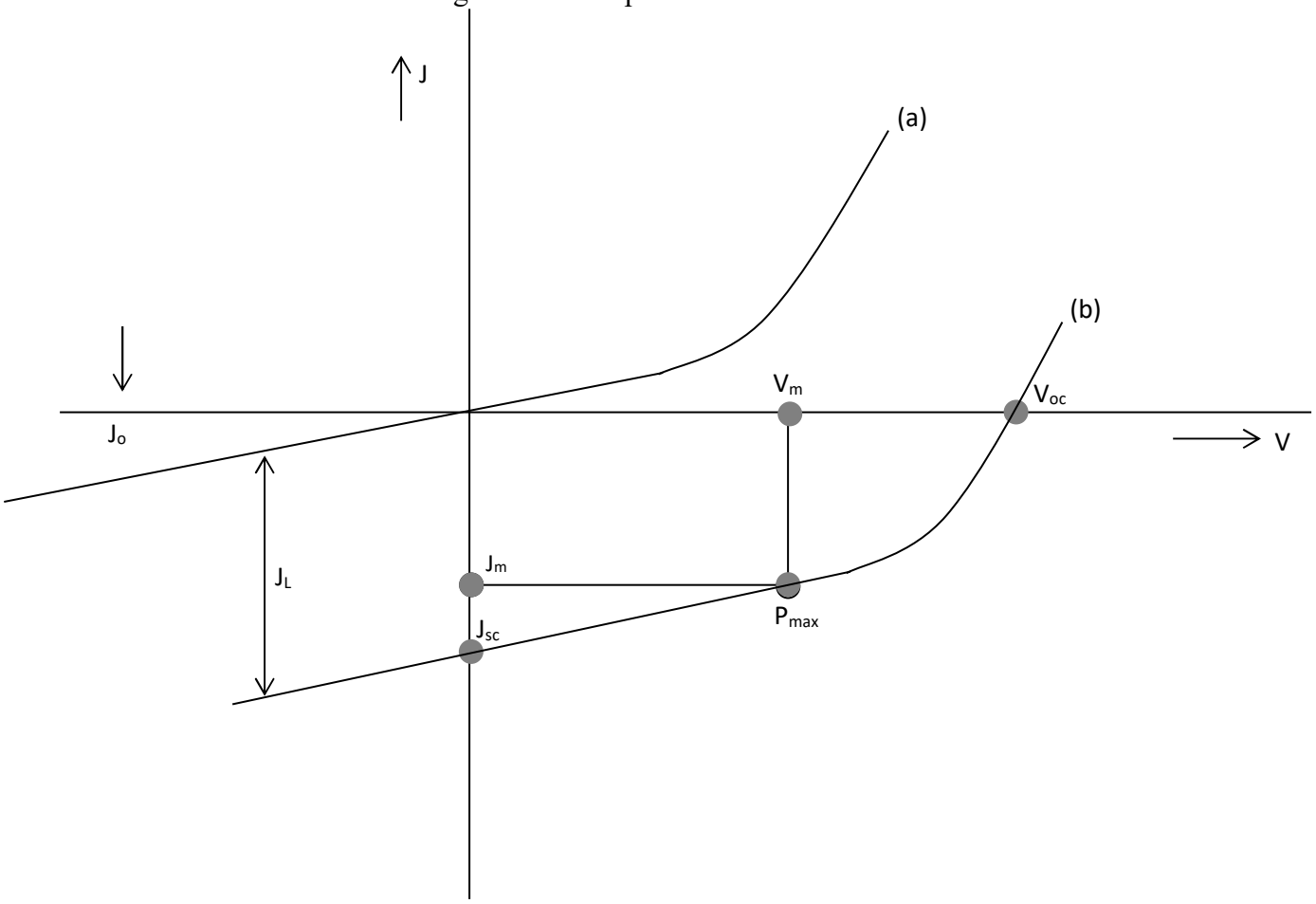

Fig. 2.3: Current/voltage characteristic of a solar cell (a) in the dark, and (b) under illumination

2.3 SOLAR CELL PARAMETER

The major electrical parameters of a solar cell can be analyzed by studying its current voltage characteristics under illumination and the dark. These parameters provide the output performance of solar cell and they are:

2.3.1 The Light Generating Current Density, j_L The light generated current density J_L is the current which increases with more illumination.

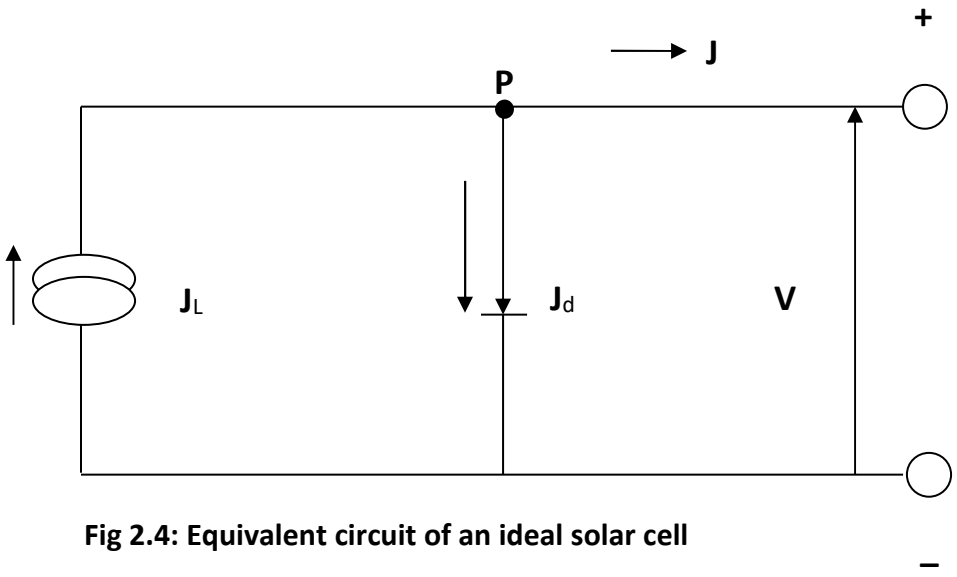

Fig 2.4: Equivalent circuit of an ideal solar cell

2.3.2 The short Circuit Current Density, J_{sc}

Is the amount of deviation along j-axis as a result of illumination. It is the current that flows through the junction under illumination at zero applied voltage (i.e. V = 0).

At point P in figure 2.4, we get that $J_L = J_d + J$ and $J = J_L - J_d$

But $J_d = J_o\left[exp\left(\frac{qV}{AKT}\right) - 1\right]$ is the diode current – voltage equation (1)

$\therefore \quad J = J_L - J_o\left[\exp\left(\frac{qV}{AKT}\right) - 1\right]$

when V = 0 (Condition at short circuit current)

$$J_{sc} = J_L - J_\circ(exp(0) - 1) = J_L - J_\circ(1 - 1)$$

$$J_{sc} = J_L \qquad (2)$$

2.3.3 The Open-Circuit voltage, V_{oc}

The open-circuit voltage of an electrical device is its voltage on open circuit. The terminal current density though the device at open circuit voltage condition is zero (i.e. J = 0).

From equation 1

$$V_{oc} = \frac{AKT}{q} \ln\left(\frac{J_{sc}}{J_o} + 1\right) \text{ and since } J_{sc} \gg J_o, \text{ then } \frac{J_{sc}}{J_o} \gg 1 \text{ then}$$

$$V_{oc} = \left(\frac{AKT}{q}\right) \ln\left(\frac{J_{sc}}{J_o}\right) \qquad (3)$$

2.3.4 The non-ideality factor, A

The diode non-ideality factor A, is also called the junction perfection factor. For a perfect junction A=1 and the open circuit voltage, V_{oc} attains its maximum value, while for higher values of A, J_o is larger such that V_{oc} reduced. The former is for solar cells that are quite large compared to conventional diodes which as well approximate an infinite plate and these usually exhibit near ideal behavior under standard Test condition. These tend to have increased V_{oc}. The later tend to erode the cell output.

2.3.5 The dark saturated current Density, J_o

The dark saturated current density, J_o is the sum of the thermally generated current in the n and p materials in the dark. It is obtained when a large negative voltage is applied across the solar cell in the dark. The dark saturated current is usually opposite in direction to the photocurrent and it therefore, tends to short the device; it is therefore desirable that J_o be as small as possible for a good solar cell.

2.3.6 Power conversion efficiency

The electrical power conversion efficiency, η of a solar cell is the ratio of the power output, P_{out} to the total power input, P_{in} of the light incident on the cell. This is expressed as:

$$\eta = \frac{P_{max}}{P_{in}} \times 100\% = \left(\frac{FF \times J_{sc}V_{oc}}{P_{in}}\right) \times 100\% \quad (4)$$

The efficiency of a solar cell can be determined from its I-V characteristic.

2.4 THEOROTICAL DETERMINATION OF SOLAR CELL ELECTRICAL PARAMETERS

Determination of the solar cell parameters requires clear understanding of the basic theory regarding the parameters. The parameters determined include Fill factor (FF), electrical power conversion efficiency (η), series resistance (R_s), shunt resistance (R_{sh}), dark saturated current density (J_o) and the non-ideality factor (A)

2.5 DEFECTS IN Cu_2O

When a crystal of compound XY is formed it is usually thought of as having equal numbers of X and Y atoms. Such a crystal is said to be stoichiometric. However, this stoichiometry is not obeyed by many solids as the ratio of atoms in them is slightly different from the ratio in one mole. Such non-stoichiometric compounds balance their structure by the presence of defects; vacancies, interstitials or both (Sear and Fortin, 1984). Cuprous oxide is one of such non-stoichiometric materials with formula $Cu_{2-\delta}O$. The deviation from stoichiometry, δ is generally attributed to some imperfections. Sears and Fortin, (1984) reported that an excess of oxygen, as a result of stoichiometry, is the major active impurity and gives as a p-doped semiconductor.

2.6 METHOD OF PRODUCTION OF Cu_2O

Many methods of producing Cu_2O have been reported in the literature. These include: thermal oxidation, electro-deposition, sputtering and chemical bath deposition.

2.6.1 Thermal oxidation

This is by far the most widely used method of producing Cu_2O for the fabrication of solar cells. The procedure involves the oxidation of high purity copper at an elevated temperature (1000 – 1,500^oC) for times ranging from few hours to few minutes depending on the thickness of the starting material (for total oxidation) and the desired thickness of Cu_2O (for partial oxidation).

The oxidation process can be carried out either in pure oxygen or in laboratory air. Cu_2O has been identified to be stable at limited ranges of temperature and oxygen pressure. It has been indicated that during oxidation, Cu_2O is formed first and after a sufficient long oxidation time, CuO is formed. However, temperature below 1000^oC and at atmosphere pressure, mixed oxide of Cu_2O and CuO are formed as observed from the X-ray diffraction (XRD) result. It has been suggested that the probable reactions that could account for the presence of CuO in layers oxidation below 1000^oC are (Musa *et al,* 1998):

$$4Cu + O_2 \longrightarrow 2Cu_2O \quad (5)$$

$$2Cu_2O + O_2 \longrightarrow 4CuO \quad (6)$$

The unwanted CuO can be removed using an etching solution containing $FeCl_3$, HCl and NaCl.

The oxidation process is followed by annealing the sample at 500^oC and then stopping the process by quenching in cold water. This process leads to good quality polycrystalline Cu_2O with

the bulk resistivity in the range $10^2 – 10^4$ Ωcm (Trivich *et al*, 1978 and Economou *et al*, 1982) using this procedure.

It is also worthy of note that the purity of the starting Cu material can have a significant impact on the quality of Cu_2O and the performance of the resulting solar cell. A number of pre- and post-oxidation treatments have been suggested in the literature (Olsen *et al*., 1982) which involves cleaning, etching, polishing and annealing the material prior to and after the oxidations.

2.6.2 Electro-deposition

Another method of producing thin films of Cu_2O is by electro-deposition. Thin films of Cu_2O can be electro-deposited by cathodic reduction of alkaline cupric lactate solution, either on metallic substrates or on treatment conducting glass slides coated with highly conducting semiconductors (Noguet *et al*, 1977).

The properties of the electrodeposited films of Cu_2O are largely similar to those prepared by thermal oxidation. The grain sizes of the electro-deposits varies from 0.1 to 10μm. The major problem, however, is in the high resistivity (10^4- 10^6 ohmcm) of the electrodeposited Cu_2O film (Economou *et. al*, 1982).

2.6.3 Sputtering

Cathode sputtering is essential one of the methods used for the preparation of thin films. The method requires very low pressure in the working space and therefore makes use of vacuum technique. The material to be sputtering is used as cathode in the system in which a glow discharge is established in an inert gas at a pressure of $10^{-5} – 10^{-6}$ torr and a voltage of a few

kilovolts. The substance on which the film is to be deposited is placed on the anode of the system.

The positive ions of the gas created by the discharge are accelerated towards the cathode (target). Under the bombardment of the ions the material is removed from the cathode (mostly in the form of neutral atoms or in the form of ions). The liberated components condense on surrounding areas and consequently on the substrate placed on the anode.

Reactive sputtering is used in the production of Cu_2O. A chemical reaction occurs with the cathode material (Cu in this case) and the active gas (oxygen) either added to the working gas or as the working gas itself. The resistivity of the deposited Cu_2O film can be controlled over a wide range by simply varying the oxygen pressure. Cu_2O films of resistivity as low as 25 ohmcm have been reproducibly obtained (Drobny and Pulfrey, 1979) by this technique.

2.6.4 Chemical Bath Deposition

The chemical bath deposition (CBD) method is one of the cheapest methods to deposit thin films and nanomaterials, as it does not depend on expensive equipment and is a scalable technique that can be employed for large area batch processing or continues deposition. The chemical bath deposition involves two steps, nucleation and particle growth, and is based on the formation of a solid phase from a solution. In the chemical bath deposition procedure, the substrate is immersed in an aqueous solution containing the precursors.

The CBD method requires only solution containers and substrate mounting devices, the one drawback of this method is the wastage of solution after every deposition. Among various

deposition techniques, chemical bath deposition yield stable, adherent, uniform and hard films with good reproducibility by a relatively simple process. The chemical bath deposition method is one of the suitable methods for preparing highly efficient thin films in a sample manner. The growth of thin films strongly depends on growth conditions, such as duration of deposition, composition and temperature of the solution, and topographical and chemical nature of the substrate.

2.7 FABRICATION OF HETEROJUNCTION SOLAR CELLS OF Cu_2O

A heterojunction solar cell is fabricated by depositing n-type semiconductor of suitable band gap on Cu_2O. Methods like vacuum deposition, sputtering and electrodeposition have been used for the deposition. Several heterojunction solar cell structures have been studied and report (Herion *et al,* 1980). Examples are the zinc oxide-cuprous oxide (ZnO/Cu_2O) and cadmium oxide-cuprous (CdO/Cu_2O) solar cells.

Transparent conducting metal oxides, being n-type were used extensively in the production of heterojunction cells using p-type Cu_2O. Herion *et al,* 1980, have reported on a fairly detailed study of ZnO/Cu_2O devices. This was achieved due to the interest they had on metal oxides being generally stable compounds and the assumption that they are not likely to react with Cu_2O. Eventually, the cell exhibited poor performance. The cell characteristics were clearly influenced by the copper rich region adjacent to Cu_2O substrate. It was finally concluded that ZnO/Cu_2O heterojunction is essential Cu/Cu_2O Schottky cell since Zn reduces Cu_2O to Cu. Hence reaction occurs with this type of cells too. Indium Tin Oxide (ITO) devices prepared by different techniques on Cu_2O were also reported (Herion *et al,* 1980 and Georgieva and Ristov, 2002). In all cases resistivity was found to be high and efficiency very low. Tanaka *et al*, (2004), have

reported an intensive work on Cu_2O prepared with TCOs. They used TCO thin films such as indium oxide (In_2O_3), tin oxide (SnO_2) and multicomponent oxides like Aluminium-Zinc- oxide (AZO) and aluminium- zinc- indium- tin- oxide (AZITO), in addition to ZnO. Highest efficiency of 1.2% was obtained with AZO-Cu_2O devices prepared at 150^0C and measured under air mass 2 (AM2) illuminations. Others yielded disappointing results. A better cell was reported by Trivich *et al.,* 1981. Using CdO it was found to generate an open circuit voltage, V_{oc}=0.4V and short circuit current, I_{sc}=2mA $cm^{-2.}$

There was no reduction of the Cu_2O layer observed, which shows the absence of any chemical reaction at the CdO/ Cu_2O interface. This suggested a possibility of avoiding chemical reaction at the interface by the use of heterojunction, especially, of oxides on Cu_2O. However the best solar cell, to date using TCO thin films is a multicomponent oxide, ITO/ZnO/ Cu_2O solar cell. It was reported to have an efficiency of 2% (Mittiga *et al*, 2006).

Copper (1) sulphide Cu_2S) is another material promising for heterojunction devices for the formation of n- Cu_2O/ Cu_2S heterojunction solar cell since Cu_2S is a p-type semiconductor as grown. Works in the past were aimed at fabricating CdS/ Cu_2O heterojunction devices. Fajinmi, (2000) reported on the deposition of Cu_2S, while Varkey, 1990, reported on copper (1) sulphide/crystalline silicon (Cu_2S/c-Si) solar cells.

2.8 FABRICATION OF HOMOJUNCTION SOLAR CELLS Cu_2O

In the past the low efficiency of Cu_2O cells was attributed to the lack of n-type Cu_2O, since an approach to achieving n-type doping has not yet been fully developed. Without it, the early studies had to rely on Schottky junctions and p-n heterojunctions for photovoltaic devices, which do not provide high efficiency. However, Fernamdo and Wethasinghe, (2000), have reported the

possibility of obtaining n-type photo-responses from clean copper plates, immersed in $CuSO_4$ solution for a few days. Subsequently, Fernando et al., (2002) reported the n-type Cu_2O produced by heating copper sheets in $CuSO_4$ solution. The formation of the n-type Cu_2O on copper surface, by heating copper sheets in $CuSO_4$ solution, can be explained by the following chemical reaction (epn.7):

$$Cu^{2+} + Cu + H_2O \longrightarrow Cu_2O + 2H^+ \quad (7)$$

The long held consensus is that the best approach to improve cell efficiency in Cu_2O based photovoltaic devices is to achieve both p- and n-type Cu_2O and thus p-n homojunctions of Cu_2O solar cells.

Experimental results in achieving both conduction types in electrochemically deposited Cu_2O by varying solution pH were reported by Longcheng and Meng, (2007). This enable p-type and n-type Cu_2O to be deposited electrochemically in sequence to form a p-n homojunctions of Cu_2O. However, the first homojunctions solar cell of Cu_2O using the electrochemical method was made by Kunhee and Meng, (2009). The cell has only 0.1% efficiency due to high resistivity of the p- and n- Cu_2O layers (or substrate).

2.9 PERFORMANCE OF Cu_2O SOLAR CELLS

The observed conversion efficiency of Cu_2O cells has remained far below the theoretical value, regardless of the method of growth of Cu_2O and the mode of fabrication of the cells. The best results obtained so far are in the range of 1-2%. Many reasons have been advanced for this low performance.

Barrier height measurements in various Schottky barrier solar cells have shown that values are always in the range 0.7-0.9 eV regardless of the metal except for the case of gold and silver which form Ohmic contacts with Cu_2O. This apparent plateau for the value of barrier height is believed to be the principle cause of the low performance of the Cu_2O Schottky barrier solar cells. Studies on schottky barrier solar cell indicate that there always exists a copper rich region at the interface between most metals and Cu_2O regardless of the choice of the metal used. All Schottky type cells are therefore essentially Cu/ Cu_2O solar cell and hence the constancy of the value of barrier height and the low electrical power conversion efficiency.

Papadimitriou *et al*, (1981), have reported the results of their study on ZnO/Cu_2O junction solar cells. The best values they obtained for open – circuit voltage (V_{oc}) were of the order of 0.3 V. A copper rich region adjacent to the Cu_2O substrate was found to be reasonable for dictation the cell characteristics. For the case of CdO/ Cu_2O heterojunction formed at room temperature, no copper metal was found at the interface. The CdO/Cu_2O cell showed a short circuit current of 2 $mAcm^{-2}$ and V_{oc} of 0.4V.

The method of electrodeposition is particularly attractive for its simplicity, low cost and possibility of making large area thin films (Wijesundara *et al*, 2006). But the resistivity of electrodeposited Cu_2O films were reported to be quite high, of the order of 10^4 – 10^6 Ωcm (Economou et al. 1982 and Wijesundara *et al*, 2000), and there, the photovoltaic properties of the solar cells made with these films were poor. Several other production techniques of Cu_2O layer were later employed in order to improve on its resistivity. The various methods include thermal oxidation (Sear and Fortin, 1984, Musa, 1995 and Mittiga *et al*, 2006), chemical vapour deposition, or radio frequency magnetron sputtering (Akimoto *et al*., 2006). However, little improvements were recorded as the efficiency was still very low, less than 2%.

Surface analyses combined with barrier height studies (Olsen *et al*, 1979, Herion *et al* 1980 and Olsen *et al*, 1982) indicate that Cu_2O Schottky barriers made with low work function metals are essential Cu/ Cu_2O cells due to reduction of the Cu_2O surface. The copper rich region essentially determines the barrier height. Auger depth profiles showed the occurrence of chemical reaction of thermodynamically more stable oxides at the interface and correspondingly to some reduction of the Cu_2O. Thallium is reported to be the only metal identified that would not reduce Cu_2O (Olsen *et al*, 1982). With 3.7 eV as its work function and theoretical value of a dark current, J_o of the order of 10^{-8} Acm^{-2}, a TI/ Cu_2O Schottky barrier has a very large theoretical efficiency. Efficiency of 10% at air mass one (AM1) would be possible. However, deposition of TI of reasonable sheet conductance is not on a substrate at room temperature. It was reported that TI of adequate sheet conductance was deposited on cool substrate. Studies on the TI/ Cu_2O barrier represented only a slight improvement over the Cu/ Cu_2O device. In fact studies on a number of metal/ Cu_2O and metal/insulator/Cu_2O contacts (Trivich *et al*, 1981) showed that the barrier height did not depend on the work function of metal.

Intensive work was done regarding deposition of Cu_2O and the dopant impurities (Musa, 1995 and Akimoto *et al*., 2006) but general observation show that the various dopants used for further lower the resistivity showed no significant improvement, with Cadmium as an exception. Nitrogen acts as a p-type dopant. Other methods of improving the resistivity of the layer were then employed. Annealing of the Cu_2O layer at moderate temperatures, as reported by Noguet *et al*, (1977), Musa *et al*, (1998) and Wijesundara *et al*, (2006), showed some improvements. Another treatment followed; which is potassium cyanide (KCN) treatment as reported by Akimoto *et al*, (2006). The above treatments yielded little improvement since the efficiency, as at the time of this report, is still not more than 2%, for Schottky Barrier Cu_2O solar cells.

The encouraging aspect of the above treatments is that, they revealed ways for further improvements. It was shown that PV properties of Cu_2O Schottky cells are significantly affected by the surface treatment and crystallinity of Cu_2O (Fernando *et al*, 2002 and Tanaka *et al*, 2004). In particular, the deposition method and conditions are important when depositing a thin film on Cu_2O sheets.

CHAPTER THREE

EXPERIMENTAL PROCEDURE

3.0 INTRODUCTION

This chapter reveal the step-by-step procedure used in arriving at copper (I) oxide, Cu_2O starting from the initial element, copper. It also explained how the Cu–Cu_2O electrochemical cell was fabricated and the measurements of open circuit voltage V_{oc} and the short circuit current I_{sc}. It also explains why the current-voltage characteristics measurement of the solar cell was measured.

For fabrication of Cu – Cu_2O photoelectrochemical solar cell it is essential for the p-Cu_2O metal oxide semiconductor to be obtained first. The procedure for obtaining this semiconductor and that for fabrication of the photoelectrochemical solar cell is given below

3.1 CUTTING AND CLEANING THE SAMPLE

High purify copper (99.97%) in the form of foils (thickness 0.1mm) were cut into standard size wafers of 3cm × 3cm, acid rinsed and then thoroughly washed with distilled water, dried and stored in clean envelops ready for high temperature oxidation

3.2 THERMAL OXIDATION

The sample of copper foil were wrapped up with tissue paper and smoothened by rubbing with the edge of a beaker to remove the kinks on the samples. The sample were cleaned by etching in dilute nitric acid, HNO_3 and rinsed in distilled water to remove any impurities on the surface of the copper. It was then dried between tissue papers.

The furnace was switched on and set to the oxidation temperature of 950ºC. It took the furnace about one hour to attain the oxidation temperature and copper sample was placed in the ceramic crucible and place inside the furnace and oxidized for eight minutes (8mins) and immediately quenched in cold distilled water. The sample was removed from the distilled water and dried by placing them between tissue papers.

The oxidized samples were annealed at a temperature of 500ºC. The annealed samples were quenched in cold distilled water and air dried.

3.3 CHEMICAL ETCHING

After oxidation and annealing has been completed a black surface of cupric oxide (CuO) is usually formed in addition to the liver red cuprous oxide (Cu_2O). The black cupric oxide was removed by chemical etching. Twenty (20) grammes of $FeCl_2$ and sixteen (16) grammes of NaCl were dissolved in 400ml of distilled water. 20ml of concentrated HCl was added to the solution, shaken carefully until the black colour is completely etched. The samples were then removed, rinsed with distilled water and dried between tissue papers and finally in air.

Another chemical etching was carried out using 8g of potassium persulphate dissolved in 160ml of the distilled water. The samples were finally rinsed in distilled water and dried between tissue papers. The etching process was considered complete when the characteristic liver red colour of Cu_2O appeared.

The black CuO layer formed during oxidation was removed when shaken in a solution of $FeCl_3$, HCl and NaCl, leaving behind the red Cu_2O.

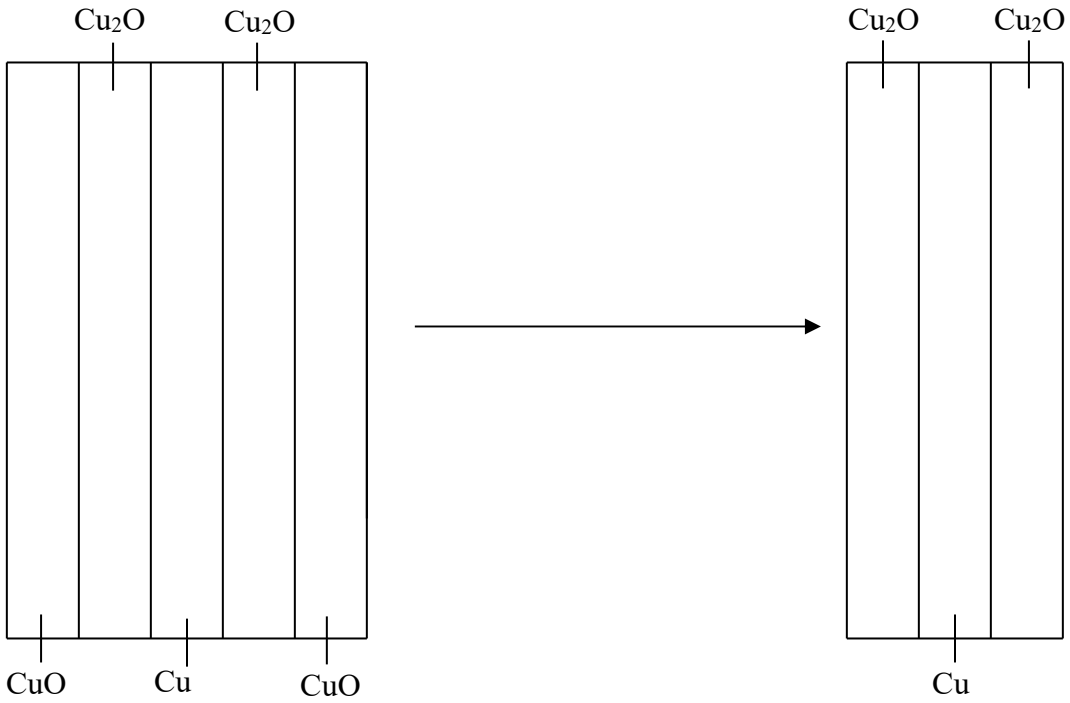

Figure 3.1: Block diagram of the etching process

3.4 CELL FABRICATION

1 mole of each electrolyte (i.e the molecular mass dissolved in 1 liter of distilled water) was poured into the transparent plastic container. Copper wire electrodes were made to the copper (I) oxide and the copper counter electrode using silver paste and both placed inside the plastic container. A complete circuit was then made by connecting the two electrodes to a micro – ammeter as illustrated in fig 3.2.

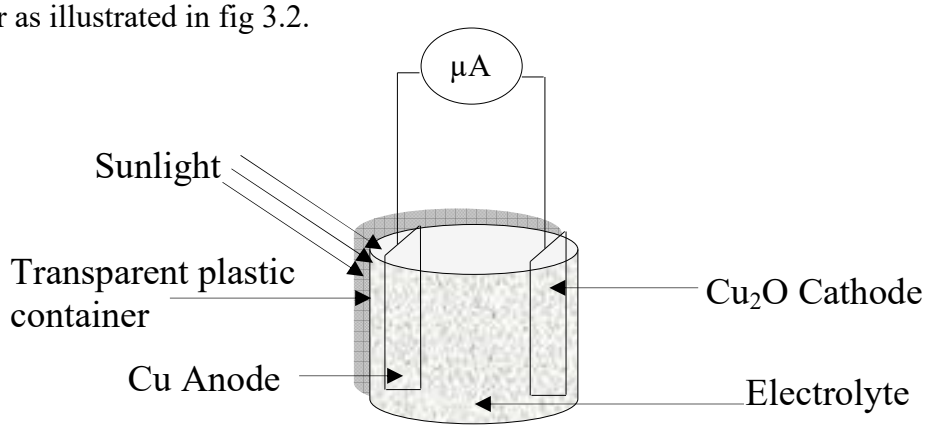

Figure 3.2: Illustration of the fabricated Cu – Cu_2O Photoelectrochemical solar cell.

3.5 MEASUREMENT OF OPEN CIRCUIT VOLTAGE AND SHORT CIRCUIT CURRENT

To understand the electron behaviour of a solar cell, it is useful to create a model which is electrically equivalent, and is based on discrete electrical component whose behaviour is well known.

Since the electrical properties of Cu/Cu_2O electrochemical solar cell depends on the intensity of sunlight, the current and the voltage were measured with a digital voltmeter under sunlight illumination for discrete time ranging from 10.00am ─ 4.00pm with 30 minutes intervals to determined the short circuit current, I_{sc} and the open circuit voltage, V_{oc} of the Cu/Cu_2O electrochemical solar cell. The I-V characteristics was determined with the aid of the experimental configuration in figure 3.3, where the resistance is being varied to acquire series of readings for the current and voltage simultaneously.

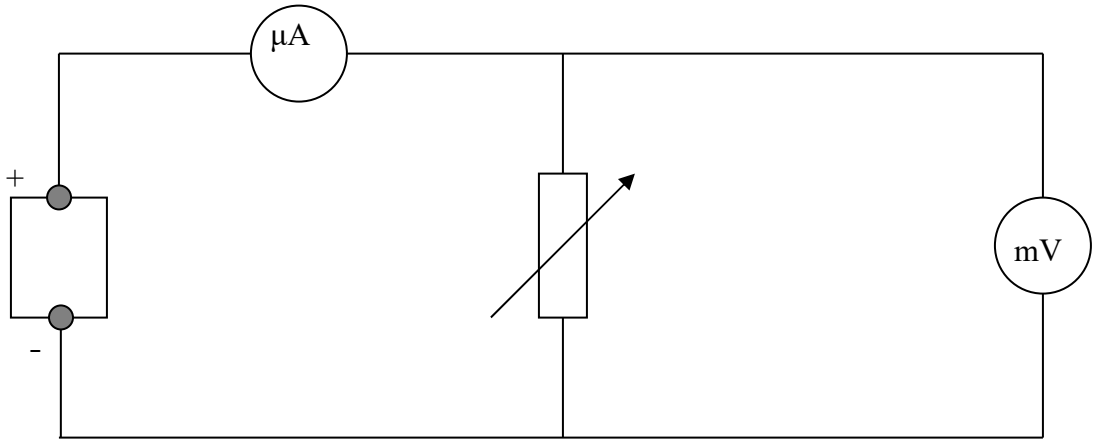

Figure 3.3 Circuit diagram of the I-V Characteristic Measurement

CHAPTER FOUR

4.1 RESULTS

The results of the I–V characteristic studies obtained for the use of the various electrolytes are given in this section

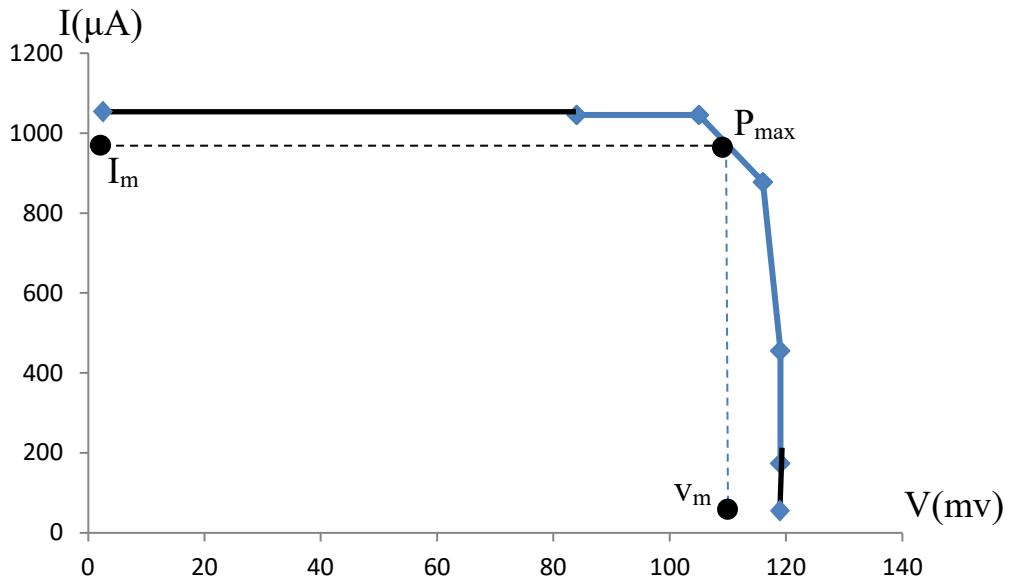

Fig 4.1 The I – V characteristic of the PEC device under illumination using $FeCl_3$ electrolyte

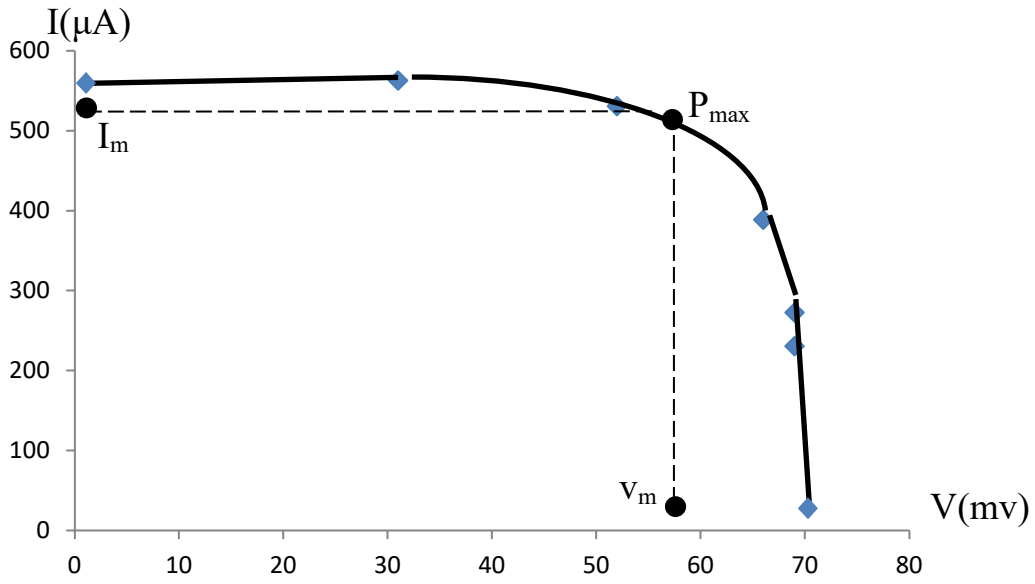

Fig 4.2 The I – V characteristic of the PEC device under illumination using NaCl electrolyte

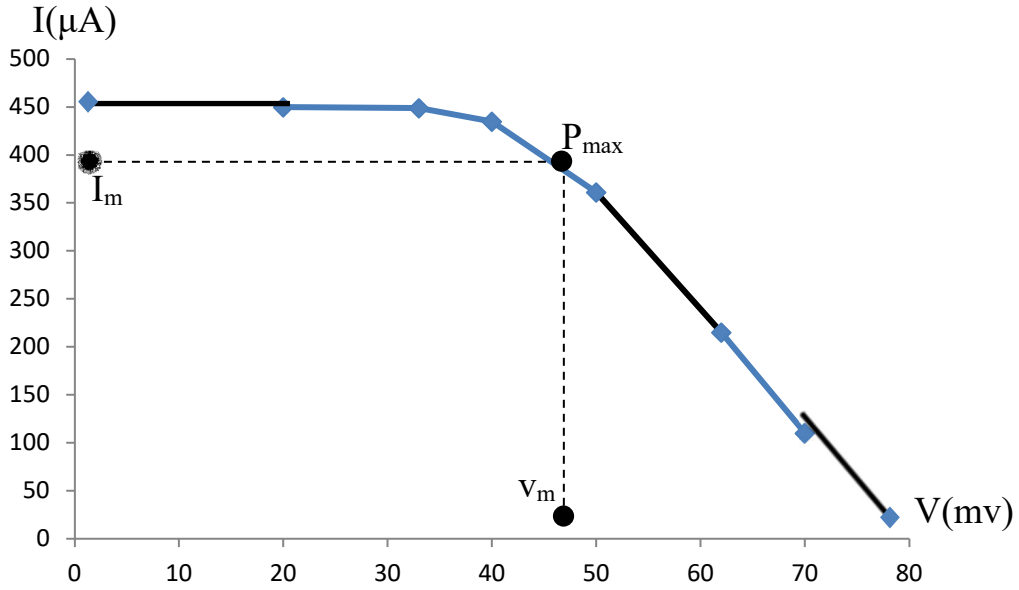

Fig4.3 The I – V characteristic of the PEC device under illumination using $BaCl_2$ electrolyte

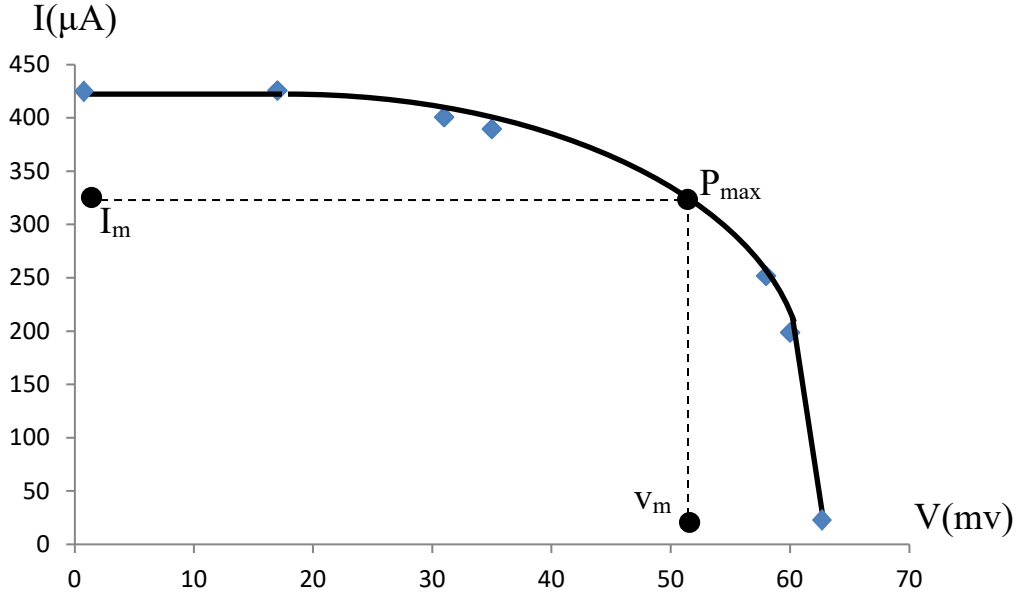

Fig 4.4 The I – V characteristic of the PEC device under illumination using $MgCl_2$ electrolyte

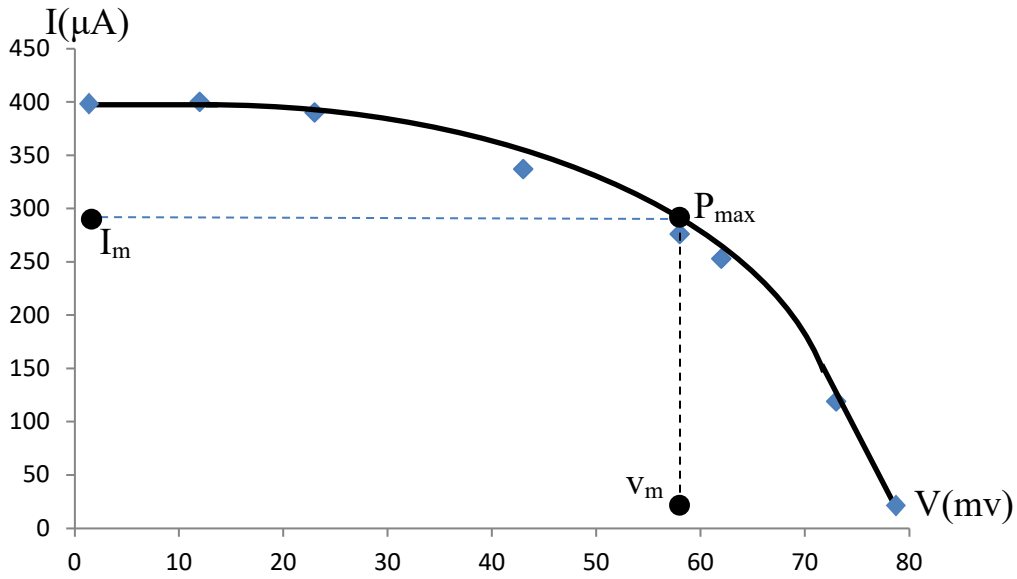

Fig 4.5 The I – V characteristic of the PEC device under illumination using$MgSO_4$ electrolyte

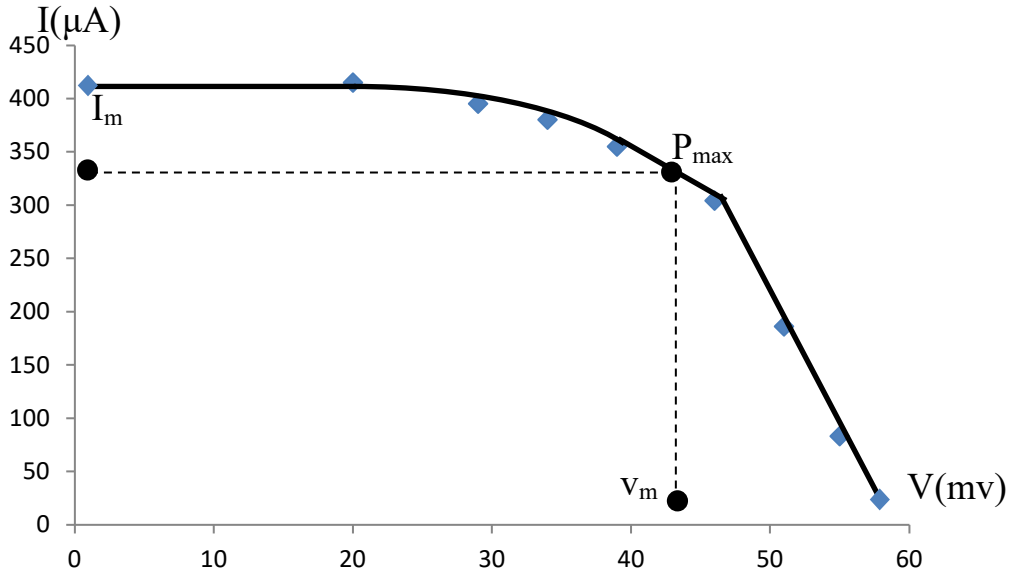

Fig 4.6 The I – V characteristic of the PEC device under illumination using KI electrolyte

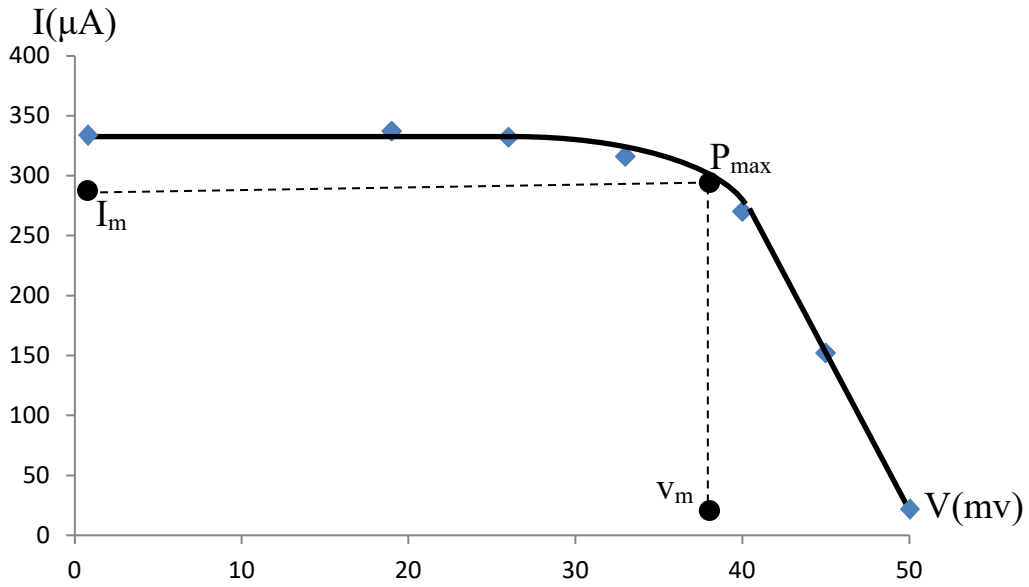

Fig 4.7 The I – V characteristic of the PEC device under illumination using $FeSO_4$ electrolyte

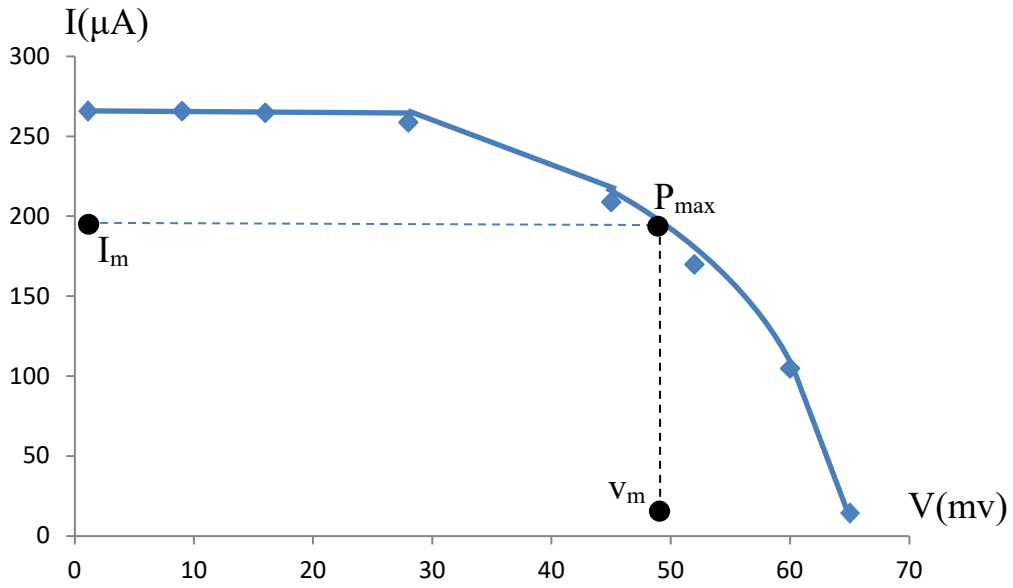

Fig 4 8. The I – V characteristic of the PEC device under illumination using $CaSO_4$ electrolyte

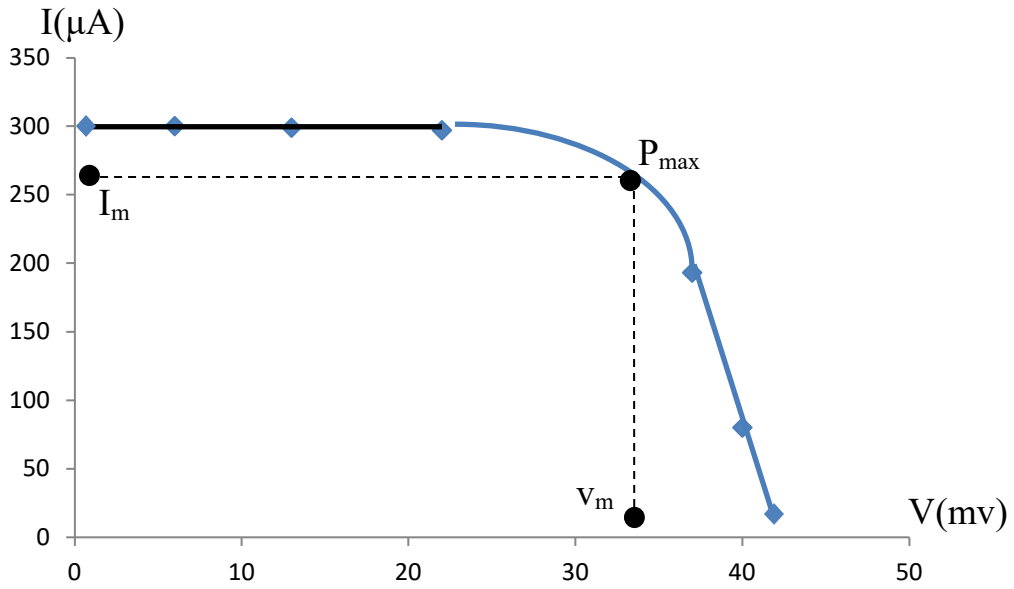

Fig 4.9 The I – V characteristic of the PEC device under illumination using $ZnSO_4$ electrolyte

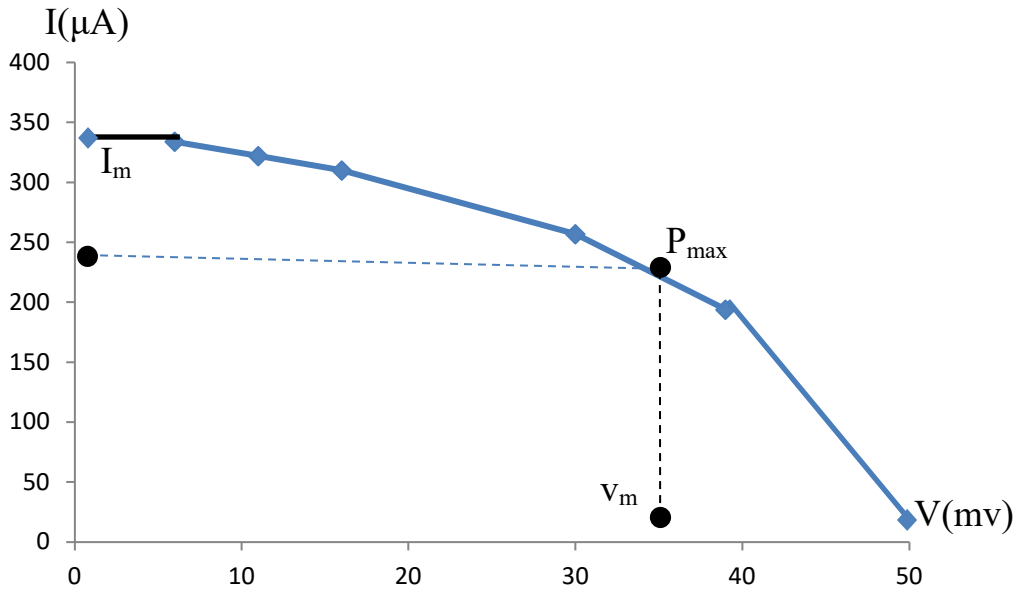

Fig 4.10 The I – V characteristic of the PEC device under illumination using $NiSO_4$ electrolyte

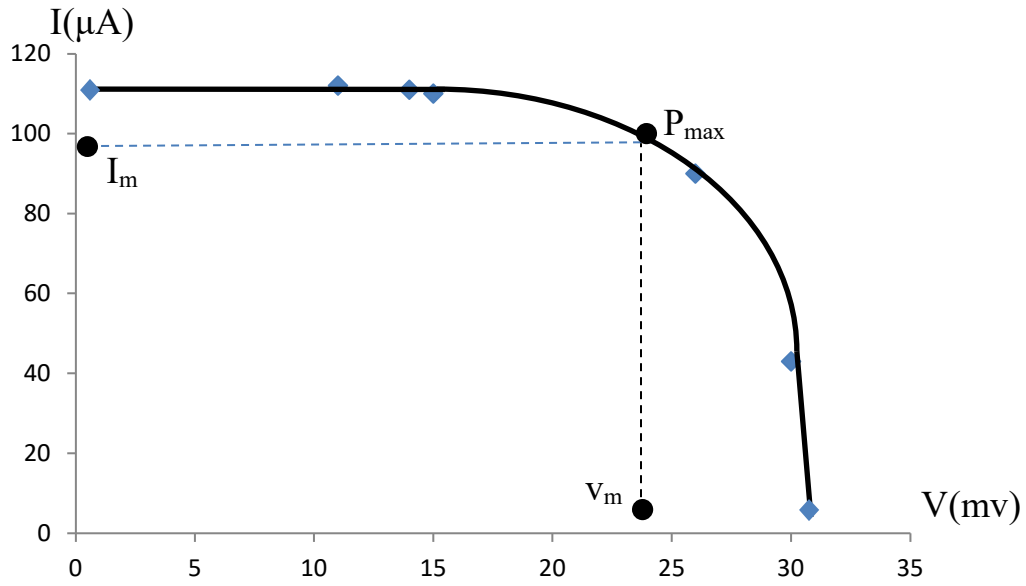

Fig 4.11 The I – V characteristic of the PEC device under illumination using $CuSO_4$ electrolyte

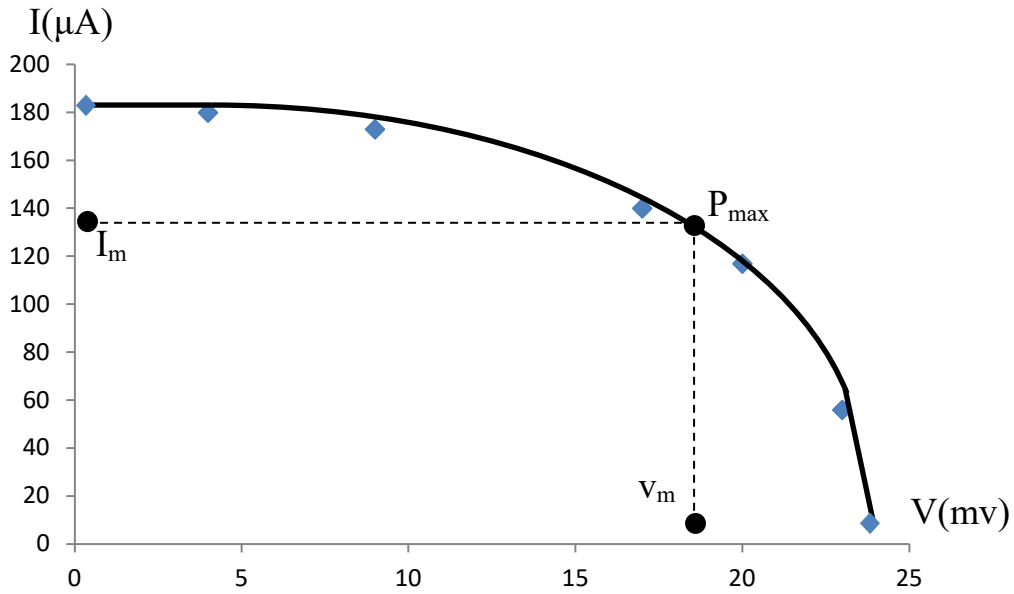

Fig 4.12 The I – V characteristic of the PEC device under illumination using $CoCl_2$ electrolyte

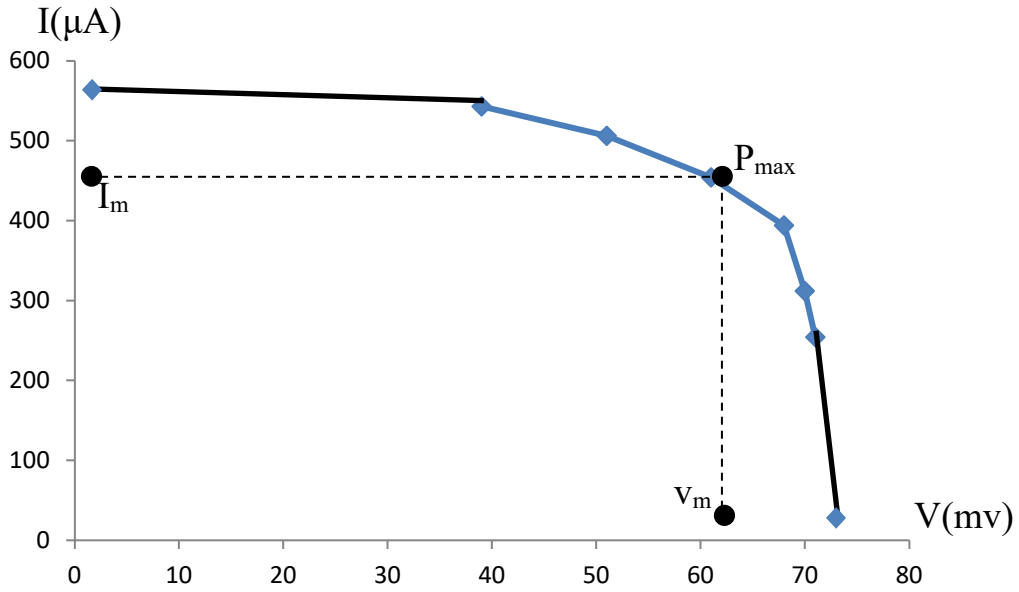

Fig 4.13 The I – V characteristic of the PEC device under illumination using a mixture of NaCl and $MgCl_2$ electrolytes.

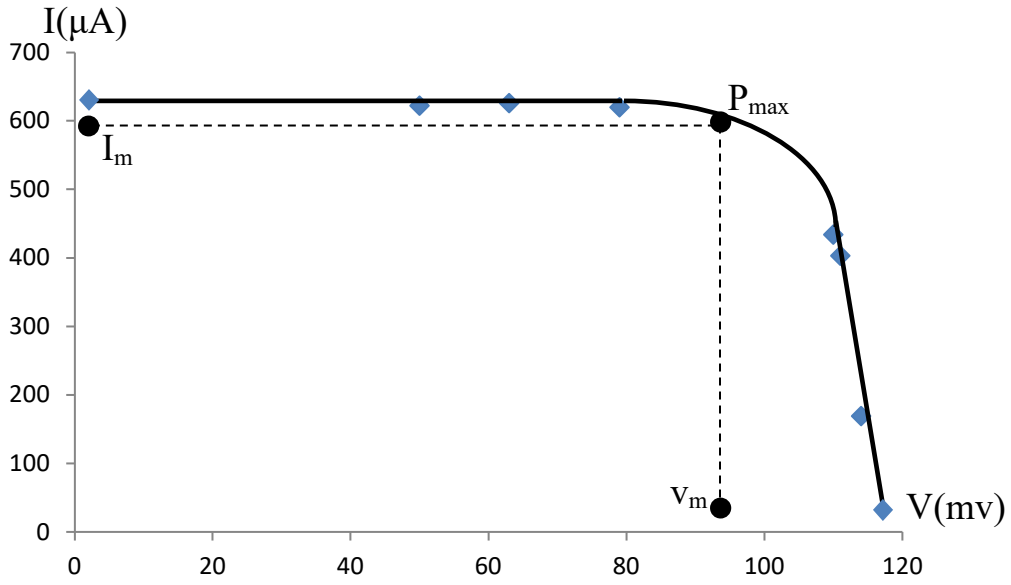

Fig 4.14 The I – V characteristic of the PEC device under illumination using a mixture of $FeCl_3$ and $NiSO_4$ electrolytes.

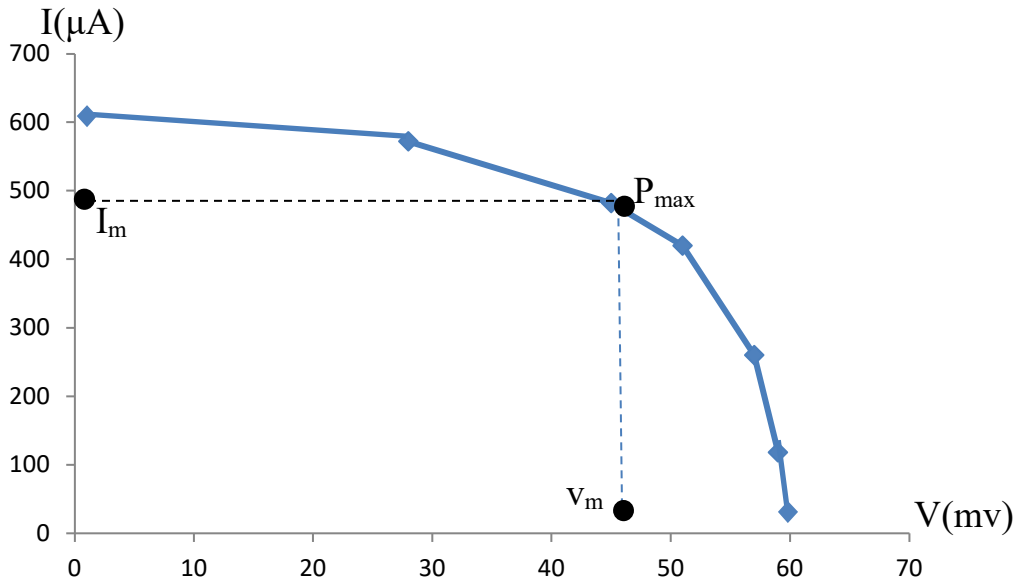

Fig 4.15 The I – V characteristic of the PEC device under illumination using a mixture $NiSO_4$ and $BaCl_2$ electrolytes.

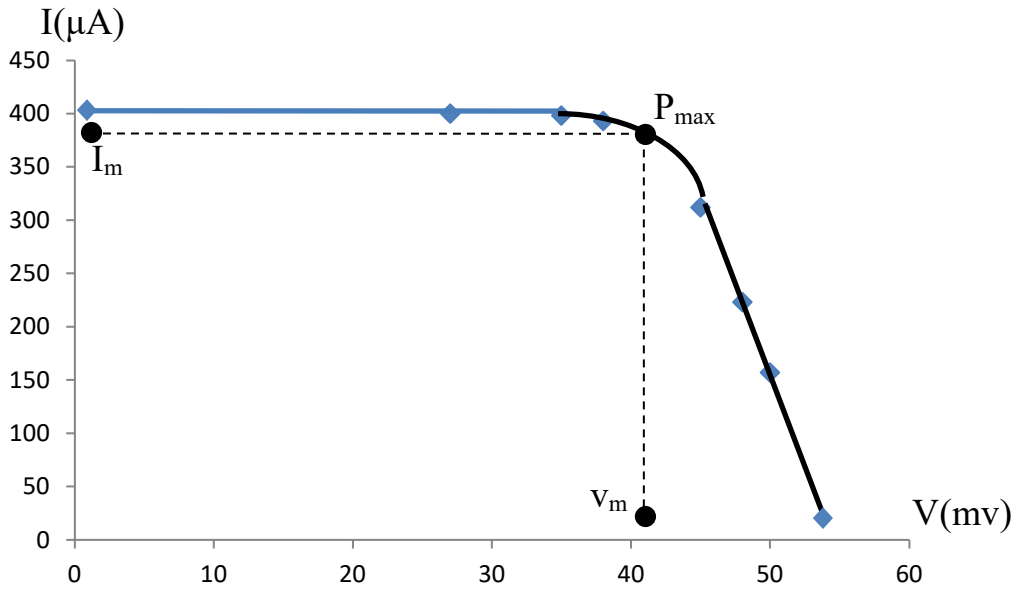

Fig 4.16 The I – V characteristic of the PEC device under illumination using a mixture of $FeCl_3$ and $BaCl_2$ electrolytes.

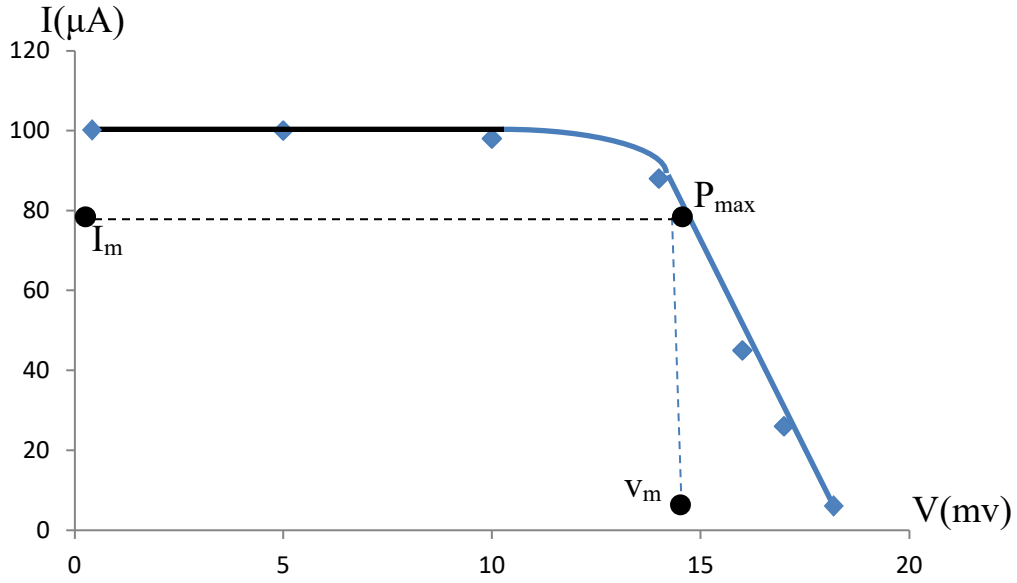

Fig 4.17 The I – V characteristic of the PEC device under illumination using a mixture of $CoCl_2$ and KI electrolytes.

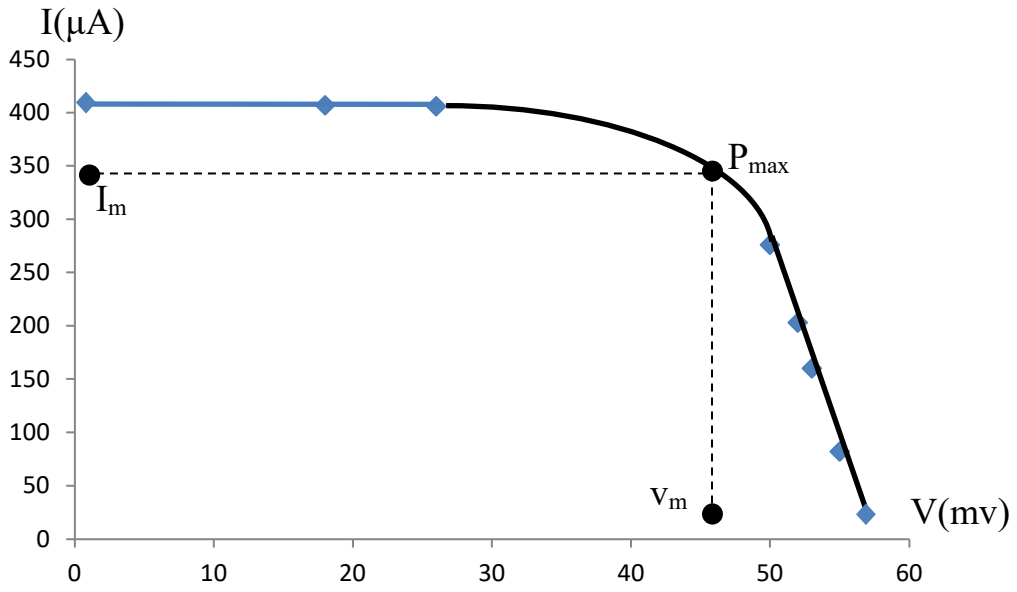

Fig 4.18 The I – V characteristic of the PEC device under illumination using a mixture of NaCl, $MgCl_2$ and $ZnSO_4$ electrolytes.

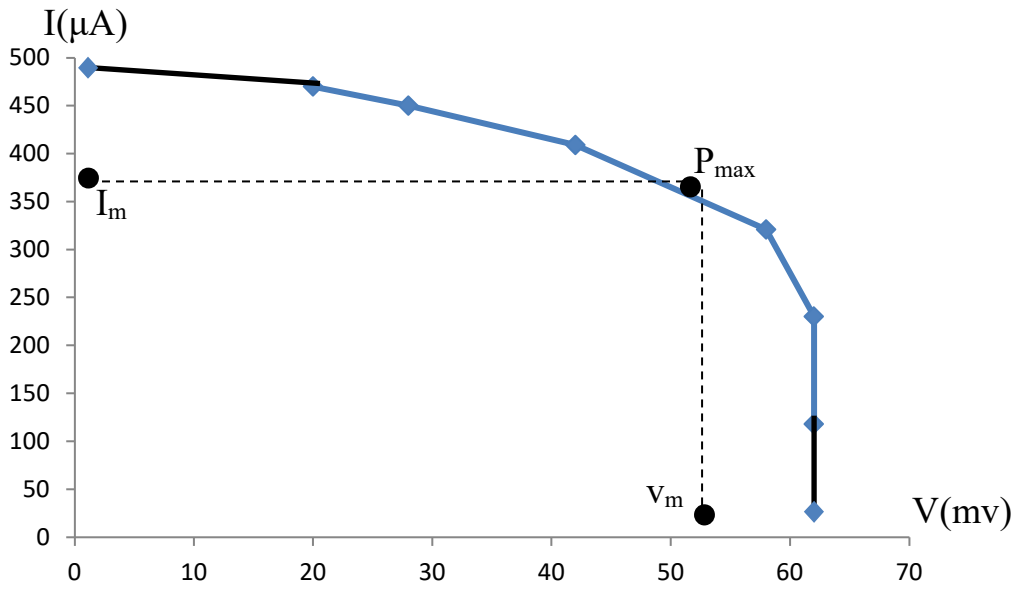

Fig 4.19 The I – V characteristic of the PEC device under illumination using a mixture of $FeSO_4$, $NiSO_4$ and $BaCl_2$ electrolytes.

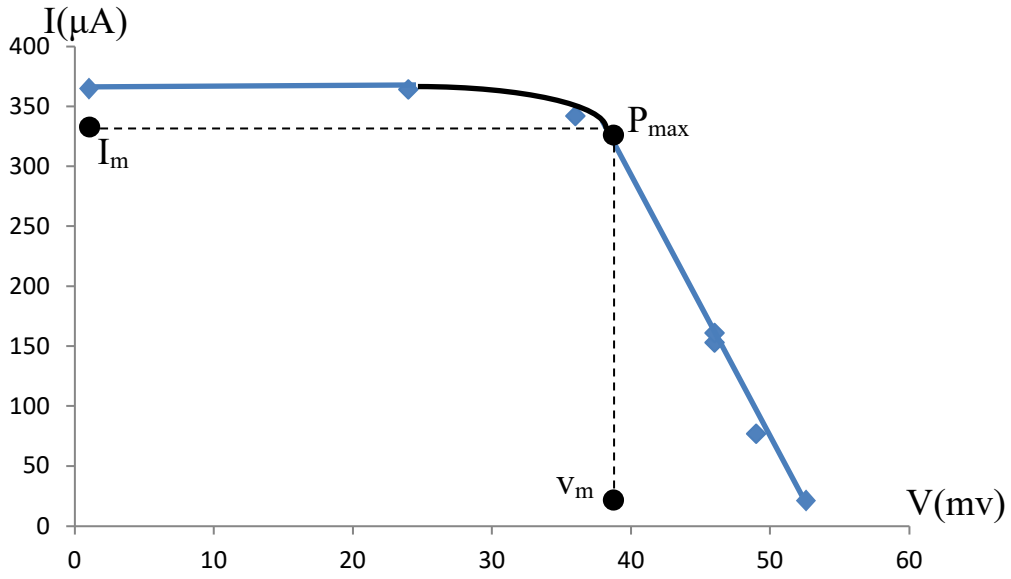

Fig4.20 The I – V characteristic of the PEC device under illumination using a mixture of NaCl, MgCl2, ZnSO4 and $CaSO_4$ electrolytes.

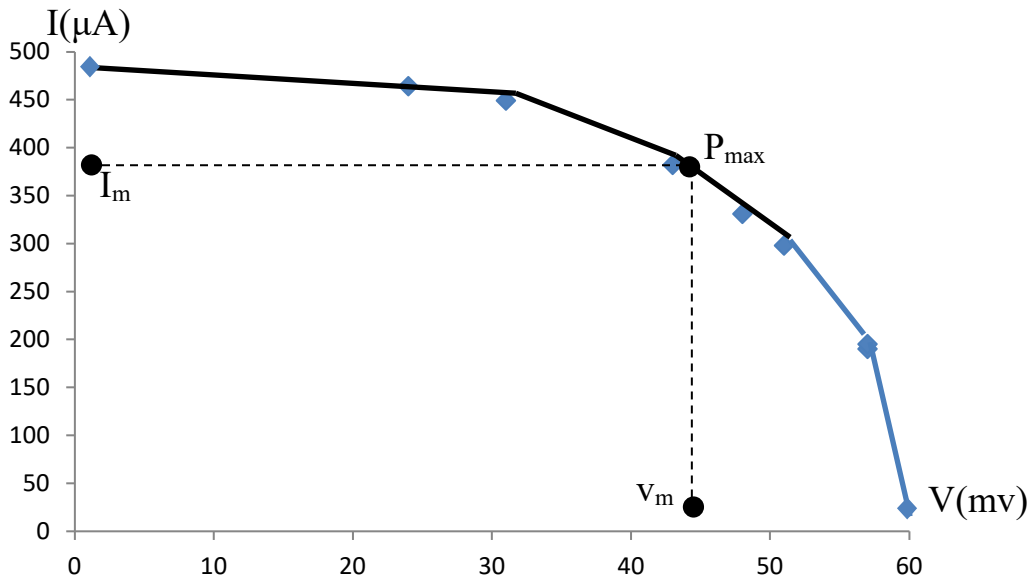

Fig 4.21 The I – V characteristic of the PEC device under illumination using a mixture of $FeSO_4$, $NiSO_4$, $BaCl_2$ and NaCl electrolytes.

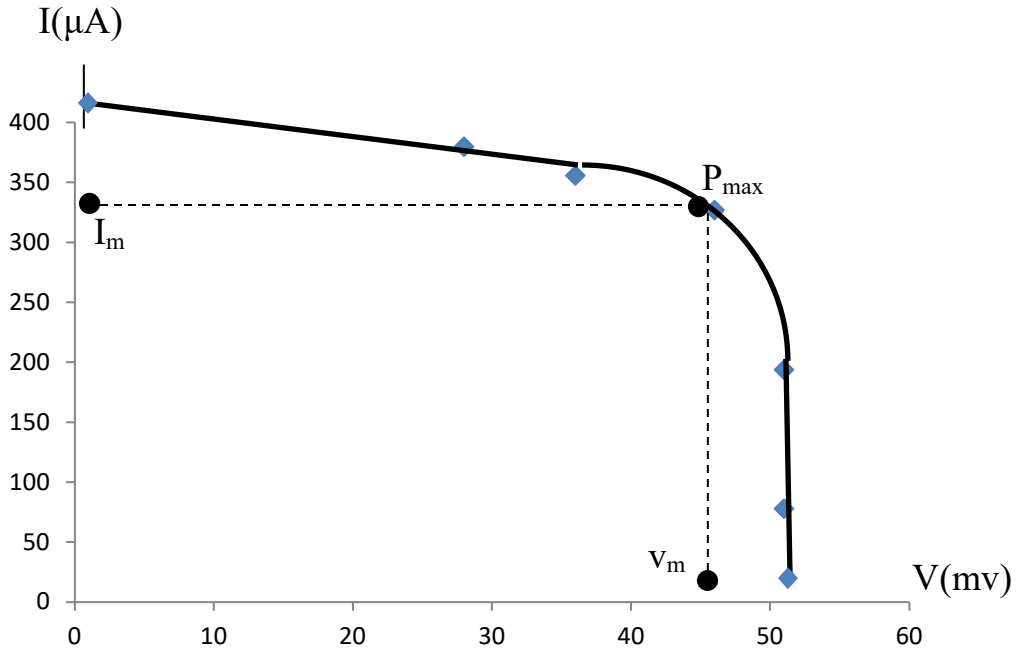

Fig 4.22 The I – V characteristic of the PEC device under illumination using a mixture of $FeSO_4$, $NiSO_4$, $BaCl_2$, NaCl and $MgSO_4$ electrolytes.

CHEMICAL REACTIONS FOR THE ELECTROLYTES USED

NaCl

Cathode $\longrightarrow H_2O_{(L)} + 2e^- \longrightarrow H_{2(g)} + 2OH^-$ (8)

Anode $\longrightarrow Cl^- \longrightarrow \frac{1}{2}Cl_{2(g)} + 1\ e^{-1}$

$CuSO_4$

Cathode $\longrightarrow Cu^{2+}_{(aq)} + 2e^- \longrightarrow Cu_{(s)}$ (9)

Anode $\longrightarrow 2H_2O_{(L)} \longrightarrow O_{2(g)} + 4H^+_{(aq)} + 4\ e^-$

KI

Cathode $\longrightarrow H_2O_{(L)} + 2e^- \longrightarrow H_{2(g)} + 2OH^-$ (10)

Anode $\longrightarrow 2I^- \longrightarrow I_{2(g)} + 2e^-$

$FeSO_4$

Cathode $\longrightarrow Fe^{2+} + 2e^- \longrightarrow Fe$ (11)

Anode $\longrightarrow 2H_2O_{(L)} \longrightarrow O_{2(g)} + 4H^+_{(aq)} + 4\ e^-$

$BaCl_2$

Cathode $\longrightarrow Ba^{2+} + 2e^- \longrightarrow Ba$ (12)

Anode $\longrightarrow Cl^- \longrightarrow \frac{1}{2}Cl_{2(g)} + e^{-1}$

$CaSO_4$

Cathode $\longrightarrow Ca^{2+} + 2e^- \longrightarrow Ca$ (13)

Anode $\longrightarrow 2H_2O_{(L)} \longrightarrow O_{2(g)} + 4H^+_{(aq)} + 4\ e^-$

$MgSO_4$

Cathode $\longrightarrow Mg^{2+} + 2e^- \longrightarrow Mg$ (14)

Anode $\longrightarrow 2H_2O_{(L)} \longrightarrow O_{2(g)} + 4H^+_{(aq)} + 4\ e^-$

$CoCl_2$

Cathode —— $Co^{2+} + 2e^{-} \longrightarrow Co$ (15)

Anode —— $Cl^{-} \longrightarrow {}^{1}/_{2}Cl_{2\,(g)} + e^{-1}$

$NiSO_4$

Cathode —— $Ni^{2+}{}_{(aq)} + 2e^{-} \longrightarrow Ni_{\,(s)}$ (16)

Anode —— $2H_2O_{\,(L)} \longrightarrow O_{2\,(g)} + 4H^{+}{}_{(aq)} + 4\,e^{-}$

$ZnSO_4$

Cathode —— $Zn^{2+} + 2e^{-} \longrightarrow Zn$ (17)

Anode —— $2H_2O_{\,(L)} \longrightarrow O_{2\,(g)} + 4H^{+}{}_{(aq)} + 4\,e^{-}$

$MgCl_2$

Cathode —— $Mg^{2+} + 2e^{-} \longrightarrow Mg$ (18)

Anode —— $Cl^{-} \longrightarrow {}^{1}/_{2}Cl_{2\,(g)} + e^{-1}$

4.2 DISCUSSTIONS

The values obtained for the short circuit current, the open circuit voltage and the fill factor are low. The major problem usually encountered in the fabrication of these class of solar cells is the series resistance (>200Ω) even after the annealing process (Musa, *et al*., 1998). This high series resistance is the major contributory factor in obtaining the low values of the short circuit current, the open circuit voltage, the fill factor and the electrical power conversion efficiency as shown in table 4.1 ranging from figure 4.1 to figure 4.22 (i.e., $3.80 \times 10^{-3}\%$ to $0.60 \times 10^{-3}\%$) for fabricated PEC solar cell. The value of power conversion efficiency is comparable with that obtained for fabrication and study of the electrical properties of Cu – Cu_2O photoelectrochemical

solar cell (Musa and Yunusa, 2013) and for backwall Schottky barrier solar cells (Musa, *et al*., 1998). The best solar cell characteristics for the backwall solar cell were obtained for thin film Cu_2O layer on copper (<15μm) (Abdu and Musa, 2012). Because they are made of direct band gap materials, the copper (I) oxide layer will be required to have thickness below <5μm for optimum performance. The major attention would have to be directed towards obtaining homogeneous Cu_2O layer of thickness of the order of 5μm and below (<5μm). The best results obtained so far are in the range of 1-2%. Many reasons have been advanced for this low performance.

Figure 4.1 is the I – V characteristic of the PEC device under illumination using $FeCl_3$ electrolyte has maximum values of internal parameters of solar cell such as; I_m, V_m, η, and P_{max} more than all electrolytes used due to the nature of the graph I_{sc} and I_m are too close to each other also V_{oc} and V_m are closed, these parameters determine the fill factor (FF) of the cell and is the ratio of the maximum output power that can extracted from the cell to the product of I_{sc} and V_{oc} and is a measure of the "squareness" of the I – V curve is also essential a measure of quality of the solar cell. FF can also be interpreted graphically as the ratio of the rectangle areas depicted in all figures ranging from 4.1 to 4.22, in Fig 4.2. Fig 4.3, Fig 4.5, Fig 4.6, Fig 4.7, Fig 4.8, Fig 9, Fig 4.10, Fig 4.11 and Fig 4.12 are those without mixture of electrolytes with values closer to that of Abdu and Musa, 2012. While table 4.1 summarized some of the most important parameters of solar cells and present what is happening to the mixtures of the electrolytes where among those without combination has maximum values which is $FeCl_3$ electrolyte followed by two, three, four, five mixtures of the electrolytes in this order. The current ─ voltage characteristic was taken under illumination and the internal parameters of the solar cell were obtained as indicated in the table below shows the electrolyte performance, using the month mean daily radiation for

Kano state compared to the work of Musa and Yunusa, 2013 even though there is differences in the amount of radiation used, temperatures differences in obtaining the p-type Cu_2O layers but in the experimental procedure have the same size of 3cm × 3cm their outcomes are; I_{sc} = 200.2μA, V_{oc} = 256mV, η = 6..9 × 10^{-2}% while my research show that $FeCl_3$ electrolyte is the best electrolyte used more than NaCl electrolyte with solar cell parameter values as follows; I_{sc} = 1117μA, V_{oc} = 118mV, η = 3.80 × 10^{-3}%. This research show that $FeCl_3$ electrolyte will gives higher value of solar cell parameters than NaCl from the comparison of the two results.

Table (4.1) Summary of results for I_m, V_m, η, and P_{max}

S/N	Type of electrolyte	I_m (μA)	V_m(mV)	Efficiency($\times 10^{-3}$%)	P_{max}($\times 10^{-4}$W)
1	$FeCl_3$	980	108	3.80	1.06
2	NaCl	540	59	1.14	0.32
3	$BaCl_2$	390	48	0.60	0.19
4	$MgCl_2$	320	51	0.59	0.16
5	$MgSO_4$	285	57	0.58	0.16
6	KI	330	43	0.76	0.14
7	$FeSO_4$	295	37	0.39	0.10
8	$CaSO_4$	188	47	0.32	0.09
9	$ZnSO_4$	256	32	0.94	0.08
10	$NiSO_4$	236	34	0.88	0.08
11	$CuSO_4$	92	23	0.76	0.02
12	$CoCl_2$	132	18.5	0.88	0.02
13	NaCl + $MgCl_2$	465	60	1.00	0.28
14	$FeCl_3$ + $NiSO_4$	550	96	1.19	0.53
15	$NiSO_4$ + $BaCl_2$	470	46	0.78	0.22
16	$FeCl_3$ + $BaCl_2$	375	41	0.55	0.15
17	$CoCl_2$ + KI	76	12.5	0.34	0.09
18	NaCl + $MgCl_2$ + $ZnSO_4$	348	43.5	5.43	0.15
19	$FeSO_4$ + $NiSO_4$ + $BaCl_2$	360	53	0.68	0.19
20	NaCl + $MgCl_2$ +$ZnSO_4$+ $CaSO_4$	316	39.5	0.45	0.12
21	$FeSO_4$ + $NiSO_4$ + $BaCl_2$ + NaCl	380	44	0.60	0.17
22	$FeSO_4$ + $NiSO_4$ + $BaCl_2$ + NaCl + $MgSO_4$	330	46	0.54	0.15

CHAPTER FIVE

CONCLUSION AND SUGGESTION FOR FUTURE WORK

5.0 SUMMARY

This research focuses attention on direct conversion of solar energy to electricity, using photovoltaic cells. The direct conversion of solar energy to electricity is likely to be a good solution to the global energy problem; especially if practical economic means of direct conversion can be developed. Africa having enjoyable high level of insolation most times of the year stands to benefit a lot from solar photovoltaic technology. Photovoltaic systems have several advantages; they are cost effective alternative in areas where extending utility power line is very expensive; they have no moving parts and require little maintenance; and they produce electricity without polluting the environment.

The theory of solar cells explains the process by which light energy in photons is converted into electric current when the photons strike a suitable semiconductor device. The theoretical studies predict the fundamental limits of solar cell, and give guidance on the phenomena that contribute to losses and solar cell efficiency.

Copper (I) oxide is prepared by partial thermal oxidation of copper foils at 950°C, annealing at 500°C then followed by chemical etching and cell fabrication where Cu_2O was used as one electrode while Cu was used as the counter electrode. 1 mole of each electrolyte was poured into the transparent plastic container. A complete circuit was then made by connecting the two electrode to a micro – ammeter this how Cu – Cu_2O Photoelectrochemical solar cell was fabricated.

Determination of the solar cell parameters requires clear understanding of the basic theory regarding the parameters. The parameters determined include Fill factor (FF), electrical power conversion efficiency (η), series resistance (R_s), shunt resistance (R_{sh}), dark saturated current density (J_o) and the non-ideality factor (A).

5.1 CONCLUSION

Photoelectrochemical solar cell of Cu–Cu_2O was successfully fabricated after partial thermal oxidation of high purify copper foil at elevated temperature it has bee shown that p-type Cu_2O layers of adequate properties for photoelectrochemical can be produced. Photocurrents and photo-voltages were recorded for most of the electrolytes used with some not giving any photocurrent readings. A comprehensive theoretical survey of the equations of photovoltaic energy conversion using the appropriate equivalent circuit diagram was given. The I – V characteristic curves were plotted for the various PEC devices and their maximum power points where calculated. The maximum power point was recorded for the $FeCl_3$ electrolyte with P_{max} $=1.06\times10^{-4}$ W and the least value was observed for the $CuSO_4$ electrolyte with $P_{max}= 2.0 \times10^{-6}$ W.

REFERENCES

Abdu, A .Y. and Musa, A. O., (2012). "Electroless Deposition and Characterization of n-Cu_2O layer, Bayero Journal of pure and applied Science, Vol.5(1)pp 1-10

Akimoto, K. Ishizuka, S Yanagita, M. Nawa, Y. Paul, K.G. Sakurai, T. (2006). Thin Film Depostion of Cu_2O and Application for Solar Cells. Solar energy, 80; 715 – 722.

Avrutin.V., (2011). "Semiconductor solar cells: Recent progress in terrestrial applications," Superlattices and Microstructures, vol. 49, pp. 337-364

Drobny, V.F and Pulfrey, D.L. (1979): Properties of Resistively-Sputtered Copper Oxide Thin Films. Thin solid films, 61: 89-98.

Economou, N.A., Toth, R,S., Komp R.J. and Trivich, D. (1982). Photovoltaic cells of electrodeposited cuprous oxide. 14th IEEE Photovoltaic Spec. Conf. Proc. New York: 1180-1185

Fernando, C.A.N. And Wetthasinghe, S.K., (2000). Investigation of photoelectrochemical characteristics of n-type Cu_2O Films. Solar Energy Materials and solar cells, 63: 299-308.

Fernando, C.A.N, de Silver, P.H.C. Wethasinha,S,K, Dharmadasa, I.M. Delson, T.and Simomonds, M.C (2002). Investigation of n-type Cu_2O Layers Prepared by Low Cost Chemical Method for Use in Photovoltaic Thin Film Solar Cells. Renewable energy, 26: 521 – 529

Green M.A., (1982). Solar Cells: Operating principles, Technology and system Applications,

Herion, J., (1979). Chemical Origin of the Space-Charge Layer in Cuprous Oxide Front-wall Solar Cells. Appl. Physics Letters: 34(9).

Herion, J, Niekisch, E.A. and Scharl, G., (1980). Investigation of Metal Oxide/Cuprous Oxide Heterojunction Solar Cells. Solar energy materials 4: 101 – 112

Longcheng, W. and Meng, T. (2007). Fabrication and Characterization of p-n Homojunctions in Cuprous Oxide by Electrochemical Deposition. Electrochemical and Solid State Letters, 10 (9): H248-H250

Mairaj A, Omar K, Arvind., (2010). Alternative Solar Cells and Their Implications. pp.14-21.

Mittiga, A. Salza, E. Sarto, F. Tucci, M. and Vasanthi, R. (2006). heterojunction Solar Cell with 2% Efficiency based on a Cu_2O Substrate Applied physics letters, 88: 163 502-1 – 163502-2

Miyake K, Uetani Y, Seike T, Kato T, Oya K, Yoshimura K, Ohnishi T (2010). Development of next generation organic solar cell.R&D Report, "SUMITOMO KAGAKU", Vol. 2010–1.

Musa, A.O. and Yunusa, A., (2013). "Fabrication and study of the electrical properties of Cu-Cu_2O photoelectrochemical solar cell", Bayero Journal of Physics and Mathematical science/vol. 5(1)pp 37-45

Musa, A.O. (1995). Development of Thin Film Copper (1) Oxide for Backwall Schottky barrier Solar Cells, Ph.D Thesis, University of Ilorin, Nigeria. 85-87, 185.

Musa A.O, (2010). "Principles of photovoltaic Energy Conversion", Ahmadu Bello, Zaria University press, Samaru, Zaria.

Musa, A. O. Akomolafe, T. and Carter, M. J. (1998). Production of Cu_2O Solar CellMaterial, by Thermal Oxidation and Study of its Physical and Electrical Properties. Solar Energy materials and solar cells, 51: 3-4.

Nouguet, C., Tapiero, M., Schwab, C. and Zielinger, J. P., Trivich, D., Komp, R. J., Wang, E. Y., and Weng, K; (1977). Cuprous Oxide as a photovoltaic Converter. 1st European Community Conf. Proceedings:1180.

Olsen, L.C. and Bohara, R. C. (1979). Explanation for Low Efficiency Cu_2O Schottky Barrier Solar Cells. Applied physics letters, 34(1): 47 – 49.

Olsen, L. C. Addis F.W. and Bohara, R. C. (1980). Solar CellI. 14th IEEE photovoltaic Specialist Conf. Proc., IEEE,New York, , p. 462.

Olsen, L.C. Addis, F.W. and Miller, W. (1982). Experimental and theoretical Studies of Cu_2O Solar Cells. Sol. Cells, 7: 247 – 279.

Papadimitriou, L. Economou, N.A. and Trivich. D. (1981). Heterojunction Solar Cells on Cuprous Oxide. Solar cells, 3: 73 – 80.

Sear, W.M. and Fortin, E.J. (1984). Preparation and Properties of Cu2O/Cu Photovoltaic Cells. Solar Energy materials, 10: 93 – 103.

Seyed, A.J., (2013). Electro Deposition of Cuprous Oxide for Thin Film Solar Cell Applications, pp. 04– 39

Stephen, J.F.(2010). Solar cells Deices physics, 2nd edition, Elsevier.

Sze S.M, (1981). Physics of semiconductor devices. John Wiley and Sons., 790-835. Tanaka, H. Shimakawa, T. Miyata, T. Sato, H. and Minami, T. (2004). Electrical and Optical Properties of TCO- Cu_2O Heterojunction Devices. Thin solid films,469-470: 80-85.

Tanaka, H. Shimakawa, T. Miyata, T. Sato, H. Minami, T. (2004). Electrical and Optical Properties of TCO-Cu2O Heterojunction Devices. Thin solid films, 469 – 470: 80 – 85.

Trivich, D., Wang, E. Y. Komp, R.J. KaKar, A.S. (1978). Cuprous Oxide Photovoltaic Cells. 13th IEEE Photovoltaic Specialist Conf. Proc. 174

Trivich, D., (1981). Heterojunction Solar Cells on Cuprous Oxide. Solar cells. 3: 73-80.

Wijesundara, R.P., Perera, L.D.R.D. Jayasuriya, K.D., Siripala W., De Silva K.T.L Samantilleke A.P., Dharmadasa I.M. (2000). Sulphidation of Electro-deposited Cuprous Oxide Thin Films for Photovoltaic Applications. Solar energy materials and solar cells, 61: 277-286.

Wijesundara, R.P. Hidaka, M. Koga, K. and Siripala, W. (2006). Growth and Characterization of Potentiostatically Electrodeposited Cu_2O and Cu Thin Films. Thin solid films 500: 241-246.

APPENDIX

Tables for current - voltage readings taken under illumination for various electrolytes used

Table 1 for $FeCl_3$ Electrolyte

Current (μA)	Voltage (mV)
1046.2	00.0
1046.0	81.1
1049.6	105.4
878.4	115.6
455.8	118.9
174.1	119.0
00.0	120.1

Table 2 for $CuSO_4$ Electrolyte

Current (μA)	Voltage (mV)
112.0	00.0
111.5	11.0
110.9	14.3
119.7	15.1
90.0	25.6
42.8	30.4
00.0	31.2

Table 3 for $CoCl_2$ and KI Electrolyte

Current (μA)	Voltage (mV)
100.1	00.0
100.0	5.2
97.9	10.1
88.0	13.5
45.3	16.3
26.4	17.4
00.0	18.5

Table 4 for NaCl, $MgCl_2$, $ZnSO_4$ and $CaSO_4$ Electrolyte

Current (μA)	Voltage (mV)
375.0	00.0
364.4	24.3
342.2	36.0
160.7	45.7
153.3	46.2
76.5	49.4
00.0	53.4

Table 5 for NaCl, $MgCl_2$ and $ZnSO_4$ Electrolyte

Current (μA)	Voltage (mV)
408.2	00.0
407.4	17.7
405.7	26.0
276.0	50.2
203.2	51.6
159.9	53.3
160.3	54.5
00.0	57.2

Table 6 for NaCl Electrolyte

Current (μA)	Voltage (mV)
570	00.0
563.1	31.3
531.4	52.0
379.8	66.2
273.1	67.7
231.6	70.3
00.0	71.1

Table 7 for KI Electrolyte

Current (μA)	Voltage (mV)
420.0	00.0
415.2	20.3
394.5	29.2
380.0	34.4
355.1	39.0
303.9	45.7
185.6	51.0
83.1	55.3
00.0	57.2

Table 8 for $FeSO_4$ Electrolyte

Current (µA)	Voltage (mV)
340.1	00.0
336.7	19.1
332.4	26.4
316.3	33.6
270.0	40.7
152.2	45.3
00.0	50.8

Table 9 BaCl Electrolyte

Current (µA)	Voltage (mV)
452.2	00.0
450.5	20.0
449.8	33.3
435.9	40.5
361.1	50.6
215.4	62.1
110.5	70.5
00.0	78.2

Table 10 for $CaSO_4$ Electrolyte

Current (µA)	Voltage (mV)
269.5	00.0
266.4	9.1
265.1	16.4
259.4	28.0
209.0	45.3
170.5	52.9
105.3	60.5
00.0	65.3

Table 11 for $MgSO_4$ Electrolyte

Current (µA)	Voltage (mV)
402.3	00.0
400.7	12.2
390.4	23.3
337.3	43.5
276.1	58.6
253.2	62.4
276.6	58.3
00.0	79.1

Table 12 for $MgCl_2$ Electrolyte

Current (µA)	Voltage (mV)
430.0	00.0
426.9	17.2
390.7	35.1
401.5	31.4
252.4	58.2
199.3	60.5
00.0	63.0

Table 13 for CoCl Electrolyte

Current (µA)	Voltage (mV)
180.1	00.0
180.0	4.1
173.6	9.5
117.2	20.3
56.5	23.2
140.9	17.1
00.0	24.0

Table 14 for $NiSO_4$ Electrolyte

Current (µA)	Voltage (mV)
339.4	00.0
334.3	6.1
322.6	11.2
310.8	16.6
257.4	30.5
194.2	39.9
00.0	49.0

Table 15 for $ZnSO_4$ Electrolyte

Current (µA)	Voltage (mV)
303.0	00.0
300.2	6.2
297.1	9.7
299.9	13.3
193.5	37.2
80.4	40.6
00.0	43.1

Table 16 for NaCl and MgCL Electrolyte

Current (µA)	Voltage (mV)
559.7	00.0
543.3	39.2
506.1	51.0
454.6	61.3
394.4	68.2
312.2	70.5
254.1	71.4
00.0	73.0

Table 17 for NaCl,$MgCl_2$ and $ZnSO_4$ Electrolyte

Current (μA)	Voltage (mV)
409.5	00.0
407.2	18.0
406.3	26.4
276.6	50.2
203.2	52.1
160.1	53.3
82.7	55.6
00.0	57.0

Table 18 for NaCl,MgC_2,$ZnSO_4$ and $CaSO_4$ Electrolyte

Current (μA)	Voltage (mV)
368.0	00.0
364.6	24.2
342.3	36.4
161.6	46.6
153.8	46.3
77.3	49.2
00.0	53.1

Table 19 for $NiSO_4$ and $Bacl_2$ Electrolyte

Current (μA)	Voltage (mV)
600.2	00.0
572.5	28.3
482.4	45.2
420.7	51.4
118.3	59.2
260.0	57.7
00.0	59.9

Table 20 for $FeSO_4$,$NiSO_4$ and $BaCl_2$ Electrolyte

Current (μA)	Voltage (mV)
480.4	00.0
470.6	20.0
450.9	28.8
409.3	42.6
321.2	58.4
230.6	62.2
118.2	62.5
00.0	63.3

Table 21 for $FeSO_4$, $NiSO_4$,$BaCl_2$ and NaCl Electrolyte

Current (μA)	Voltage (mV)
470.4	00.0
464.2	24.4
449.1	31.2
382.7	43.0
331.2	48.6
298.2	51.3
195.1	57.6
190.8	57.6
00.0	60.7

Table 22 for $FeSO_4$,$NiSO_4$,$BaCl_2$, NaCl and$MgSO_4$ Electrolyte

Current (μA)	Voltage (mV)
402.0	00.0
380.6	28.2
356.3	36.3
327.1	46.5
194.5	51.2
78.2	51.1
00.0	52.3

Table 23 for $FeCl_3$ and $BaCl_2$ Electrolyte

Current (μA)	Voltage (mV)
402.3	00.0
400.1	27.4
398.2	35.5
393.6	38.3
312.2	45.2
223.3	48.6
157.1	50.3
00.0	55.0

Table 24 for $NiSO_4$ Electrolyte

Current (μA)	Voltage (mV)
623.0	00.0
622.4	50.4
626.3	63.3
620.3	79.2
434.2	110.7
403.1	111.1
169.8	114.2
00.0	118.5